
Mechanical Engineering Theses

Mechanical Engineering

Summer 7-31-2019

Development of a Hybrid Residential HVAC System: an Experimental Study of a Variable Refrigerant Flow System with Ducted and Ductless Elements

Andrew C. Hernandez III
University of Texas at Tyler

Follow this and additional works at: https://scholarworks.uttyler.edu/me_grad



Part of the [Mechanical Engineering Commons](#)

Recommended Citation

Hernandez, Andrew C. III, "Development of a Hybrid Residential HVAC System: an Experimental Study of a Variable Refrigerant Flow System with Ducted and Ductless Elements" (2019). *Mechanical Engineering Theses*. Paper 7.

<http://hdl.handle.net/10950/1858>

This Thesis is brought to you for free and open access by the Mechanical Engineering at Scholar Works at UT Tyler. It has been accepted for inclusion in Mechanical Engineering Theses by an authorized administrator of Scholar Works at UT Tyler. For more information, please contact tgullings@uttyler.edu.

DEVELOPMENT OF A HYBRID RESIDENTIAL HVAC SYSTEM: AN
EXPERIMENTAL STUDY OF A VARIABLE REFRIGERANT FLOW SYSTEM
WITH DUCTED AND DUCTLESS ELEMENTS

by

ANDREW CARRION HERNANDEZ III

A thesis submitted in partial fulfillment
of the requirements for the degree of
Master of Science in Mechanical Engineering
Department of Mechanical Engineering

Nelson Fumo, Ph.D., Committee Chair

College of Engineering

The University of Texas at Tyler
August 2019

The University of Texas at Tyler
Tyler, Texas

This is to certify that the Master's Thesis of

ANDREW CARRION HERNANDEZ III

has been approved for the thesis/dissertation requirement on
July 11th, 2019
for the Master of Science in Mechanical Engineering degree

Approvals:



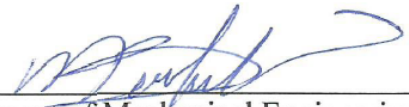
Thesis Chair: Nelson Fumo, Ph.D.



Member: Tahsin Khajah, Ph.D.



Member: Mohammad Abu Rafe Biswas, Ph.D.



Chair, Department of Mechanical Engineering



Dean, College of Engineering

Acknowledgements

I am deeply indebted to my thesis chair and mentor, Dr. Nelson Fumo. The opportunities presented to me throughout my educational career have been invaluable. The successes and educational fulfillment would not have been possible without the relentless support and profound belief in my abilities from Dr. Fumo. I would like to extend my gratitude to the professional team at the Trane Residential Heating and Cooling Research Lab at the University of Texas at Tyler for their unwavering guidance and this beneficial experience.

Table of Contents

List of Tables	iii
List of Figures	iv
Abstract	vii
Chapter 1 Introduction and Overview	1
Introduction	1
Overview	2
Chapter 2 Literature Review	6
Multi-Evaporator Air Conditioners	7
Dual Evaporator	7
Triple Evaporator	9
Four+ Evaporators	12
Multi-Evaporator Highlights	14
Refrigerants	15
Refrigerants Highlights	17
Compressors	18
Digital Scroll Compressor	18
Inverter Driven Compressor	21
Single Speed	24
Compressor Highlights	25
Thermal Comfort	26
Thermal Comfort Highlights	28
Chapter 3 Materials and Methods	29
Research Facility	29
Layout and Zoning	29
Measurement Locations	31
Sensors	34
Selection Process	34
Installation	35
Installed Hardware and Components	38
Outdoor Unit	38
ODU System Sensors	40
Indoor Units	40
Indoor system sensors	43
Data Acquisition	43
Hardware	43
LabVIEW Virtual Instruments	44
Data Access	46

Testing	46
Chapter 4 Results and Discussion.....	48
Scenario A.....	50
Scenario A'	58
Scenario B.....	61
Scenario C.....	63
Scenario D.....	64
Scenario E.....	66
Scenario F.....	67
Scenario G.....	70
Scenario H.....	73
Peripheral Data.	76
Chapter 5 Conclusions and Recommendations.....	78
References.....	80
Appendix A. Research Site.....	83
Appendix B. Indoor images	86
Appendix C. National Instruments Hardware and Software	93
Appendix D. Complete Scenario Results.....	95

List of Tables

Table 1. VRF component reference chart	6
Table 2. Location planning for data acquisition	31
Table 3. Accuracy Requirements	34
Table 4. Cooling mode testing scenario with zone target set points (SP).....	47
Table 5. General resulting data output plots	50

List of Figures

Figure 1. Diagram of the VRF HVAC components	5
Figure 2. Ductwork and HW layout.....	30
Figure 3. Spatial location planning for sensors.....	33
Figure 4. Thermocouple and RH sensor positions.....	37
Figure 5. Living room with hanging sensors	38
Figure 6. 3-ton outdoor unit	39
Figure 7. ODU refrigerant line sight glass.....	39
Figure 8. Kitchen and living room highwall unit positions	41
Figure 9. Air handler and ductwork in attic	42
Figure 10. Refrigeration pipe manifold	42
Figure 11. Sensors signal acquisition.....	45
Figure 12. Normal daily data performance (Scn. A)	50
Figure 13. Compressor speed and zone temperatures (Scn. A)	51
Figure 14. Ductless (HW) temperatures (Scn. A).....	52
Figure 15. Ducted (AHU) temperatures (Scn. A).....	53
Figure 16. Relative humidity (Scn. A).....	54
Figure 17. Demand capacity and zone temperatures (Scn. A).....	55
Figure 18. Compressor speed and superheats (Scn. A)	56
Figure 19. System state with line pressures and temperatures (Scn. A).....	57
Figure 20. Vertical temperature stratification (Scn. A')	58

Figure 21. Temperature grid along living area wall (Scn. A').....	60
Figure 22. Demand capacity and zone temperatures (Scn. B).....	61
Figure 23. Compressor speed and superheats (Scn. B).....	63
Figure 24. Two-day overall data (Scn. D)	64
Figure 25. Compressor speed and demand capacity (Scn. D)	65
Figure 26. Compressor speed and superheats (Scn. D)	66
Figure 27. Overall daily data (Scn. F).....	67
Figure 28. Demand capacity and zone temperatures (Scn. F)	68
Figure 29. System state with line pressures and temperatures (Scn. F).....	69
Figure 30. Ductless (HW) temperatures (Scn. G).....	70
Figure 31. Demand capacity and zone temperatures (Scn. G).....	71
Figure 32. Compressor speed and superheats (Scn. G)	72
Figure 33. Ductless (HW) temperatures (Scn. H).....	73
Figure 34. Demand capacity and zone temperatures (Scn. H).....	74
Figure 35. Compressor speed and superheats (Scn. H)	75
Figure 36. Daily overview of system failure and data	76
Figure 37. Troubleshooting sample	77
Figure A1. Research site signage.....	83
Figure A2. Research site with both residential houses	83
Figure A3. Front of VRF ducted-ductless HVAC system house.....	84
Figure A4. Technical floor plan of research house.....	85
Figure B1. Thermocouple hanging through acrylic tubing.....	86
Figure B2. Thermocouple positioning from ceiling	86

Figure B3. Thermocouple and relative humidity sensor.....	87
Figure B4. Master bedroom	87
Figure B5. Middle bedroom.....	88
Figure B6. Front bedroom.....	88
Figure B7. Dining room with repositionable thermocouple pole	89
Figure B8. HW3 in living room with temperature grid on wall	90
Figure B9. Airflow validation setup	91
Figure B10. Airflow measurement pressure hardware	92
Figure C1. Used cRIO modules in NI-9074 chassis.....	93
Figure C2. NI-9705 chassis with auxiliary measurement thermocouples	93
Figure C3. Data processing and forwarding VI.....	94
Figure D1. Scenario B data set	95
Figure D2. Scenario B data set (continued).....	96
Figure D3. Scenario D data set	97
Figure D4. Scenario F data set.....	98
Figure D5. Scenario G data set	99
Figure D6. Scenario G data set (continued).....	100
Figure D7. Scenario H data set	101
Figure D8. Scenario H data set (continued).....	102

Abstract

DEVELOPMENT OF A HYBRID RESIDENTIAL HVAC SYSTEM: AN EXPERIMENTAL STUDY OF A VARIABLE REFRIGERANT FLOW SYSTEM WITH DUCTED AND DUCTLESS ELEMENTS

Andrew Carrion Hernandez III

Thesis Chair: Nelson Fumo, Ph.D.

The University of Texas at Tyler
August 2019

The introduction of variable refrigerant flow (VRF) expands the range of development potential for HVAC systems. The hybridization of traditional HVAC ducted systems and ductless VRF integrates both the advantages and disadvantages of each system type. Existing research does not focus on hybridization but on individual component evaluation that covers quantitatively expansive evaporator or multiple compressor configurations. The Trane Residential Heating and Cooling Research Lab at the University of Texas at Tyler was used as the research facility to experiment and validate a hybrid ducted-ductless HVAC system where a ducted attic air handler unit and three ductless evaporator units were installed. Spatial temperature and component operation were acquired through independent data acquisition systems to report daily data based on successful evaluation scenarios. Control of the system was assessed to be done very well given the zoning layout for the indoor units. Efforts to individualize zones for the ductless components had limitations since two indoor units shared an open floor plan.

Temperature variation was found to be uniform with even one indoor unit and further balanced with addition of hybrid components with refrigerant line pressure and temperature response to compressor operation increase.

Chapter 1

Introduction and Overview

Introduction

In recent decades strides for efficiency and performance in the heating, ventilation, and air conditioning (HVAC) industry have been momentous. Where this drive comes from is the introduction of Variable Refrigeration Flow (VRF) ductless systems that are beginning to replace traditionally ducted HVAC systems in residential applications. The efficiency and performance have a number of subcategories such as compressor and superheat control alongside temperature control distribution that need to be evaluated in order to deem system developments successful. The importance of VRF systems is divided among a number of factors including improved energy efficiency, zone thermal comfort, and flexibility of design capabilities. The interest in VRF systems stems from speculation of future VRF market demand and technology advances.

The location for research and testing was held at the Trane Residential Heating and Cooling Research Lab at the University of Texas at Tyler. This site contains two houses for purposes of research and development and one of which is used for this study. The justification for the problem falls within a hybridization of the aforementioned HVAC systems. Since every HVAC system requires a different arrangement, some homeowners may not require full zone control by placing a ductless unit in every space or minimal control with a fully ducted space. The hybridization will allow the homeowner desired zone control for specific spaces while maintaining a targeted

temperature throughout the remainder of the home. Efforts in development are to bring the advantages of each system type and reduce the effect of the disadvantages. As the foundation for HVAC systems is widely known and practiced, various theory implementations will be extrapolated to this hybrid system and developed further for this system to potential hold true for hybrid VFR systems.

Overview

HVAC systems, conventionally, have been installed and operated with a complete set of airflow ductwork involved. This split system generally has the air handler unit (AHU) in an attic that supplies conditioned air to designated zones. The driving force for this refrigeration cycle is the compressor and condenser usually in a single outdoor unit (ODU). The connection between the two are refrigerant lines, which will remain similar for a VRF ductless system. The VRF system will continue to keep a similar setup with the ODU and one or more evaporator components installed in a relative high position on a wall in a specific zone. In ductless VRF systems, multiple highwall units (HW) can be installed in various zones which are to be all linked through the same refrigeration line sharing suction pressure into the outdoor unit. The hybridization for this project comes from the installation of a single AHU in the attic and three HW units throughout the research facility.

Different from the principles of a standard vapor compression refrigeration system, the refrigerant flow throughout a VRF system is controlled instead of operating at the speed of a one- or two-staged compressor setting. The set-positioned expansion valve is replaced with an electronic expansion valve (EEV) that is controlled in conjunction

with the rest of the system. An EEV is calibrated for different orifice sizes to allow any amount of refrigerant flow through to the evaporator. The positioning of the EEV orifice size is correlated to how much load is required to control zone temperature. Generally, the compressor works at a variable speed to match load required by the overall system. Energy efficiency increases since the compressor is capable at operating from a range of speeds depending on the load required to maintain temperature throughout single zone or multiple zone arrangements. Instead of a system turning on at full capacity for a brief time to cool a zone, a VRF system can turn on for the same amount of time but only at required compressor speeds that result in same zone temperature control but at lower cost due to less energy consumption.

VRF systems have a large advantage of not requiring the space a traditional split system would take to install throughout a residential environment. Reducing the required ductwork and attic space place, VRF ductless systems are high in customization. Additional to increasing efficiency and performance of HVAC systems there is a modularity factor that is included in adding refrigerant flow control. Ductless systems include a number of indoor evaporators that include the EEV and airflow fan in a compact unit all connected in parallel to the same refrigerant lines leading to and from an outdoor unit consisting of the compressor and condenser. As different zones require varying loads to maintain their desired air temperature the EEV will be told to allow more refrigerant to increase capacity to remove heat. Each of the indoor units' EEV position is communicated to the ODU, in order that the compressor operates to match the capacity provided by the flow rate.

Figure 1 shows the installed components of this hybridization of a ducted and ductless system. From the figure, the HW units are numerically labeled for the kitchen (HW1), the garage (HW2), and the living area (HW3) while remaining bedroom zones are ducted to the AHU (Main). This notation will be used throughout this study.

The vapor compression cycle has vital requirements to ensure equipment longevity and proper operation. Refrigerant entering the compressor must be superheated vapor as any liquid entered to the compressor has potential to harm the compressor internals. This is achieved by balancing the amount of warm return air introduced through the evaporator coils to evaporate the refrigerant mixture. Not enough warm airflow and the refrigerant is not capable of absorbing enough heat to fully phase change the mixture to a superheated vapor at the exit of the evaporator. Having superheated vapor ensures that the refrigerant has no liquid in the lines during this phase, so the EEV is in place to regulate refrigerant flow and allows less refrigerant to flow through and properly acquire superheated vapor. A superheat variable is considered during the reviewed investigations to monitor how effective the current refrigerant flow is. Alternatively, the airflow through the evaporator can be increased. This balance between each component within the indoor unit and compressor is how efficiency is maximized. Multiple inputs can be altered to achieve a single output. This is where controlling of the system plays a vital role in efficiency and reliability. Control is looked at overall in this study, however specific details nearing coding and logic are discussed minimally as Trane personnel receives system information after testing periods and expertly reviews changes to be made with software engineers to implement coding changes.

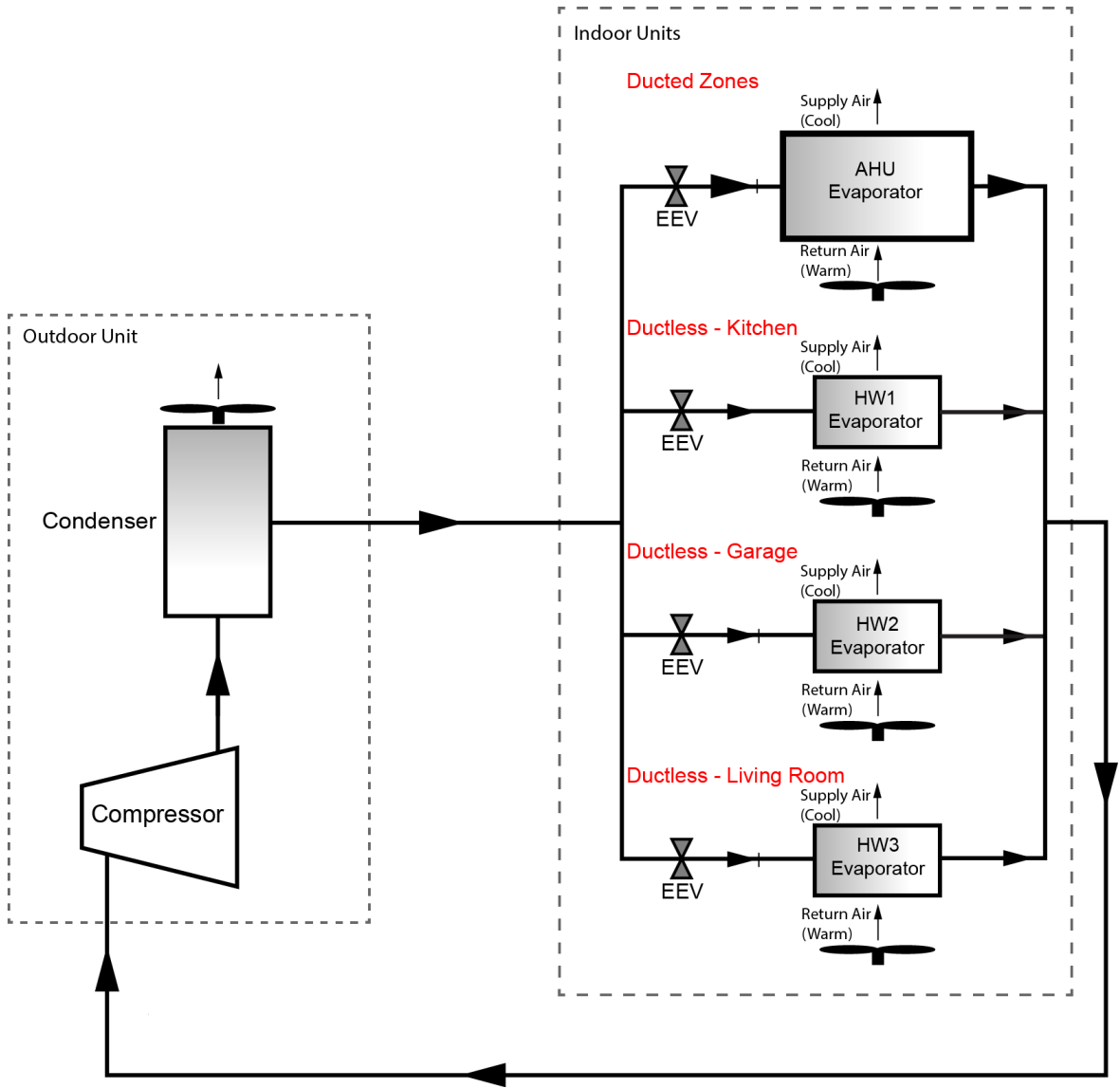


Figure 1. Diagram of the VRF HVAC components

Chapter 2

Literature Review

Trends in research specifically target performance analysis and aspects of temperature distribution independently. Findings of research for this study are deduced and synthesized in attempt to generalize conclusions to provide a comprehensive source of references material for this study. With a trailing domestic recognition for VRF, new and future studies are accommodating development in this technology. Components and categories are shown in Table 1 where information is divided to their own respective sections. Since information is plentiful from certain studies there will be overlap from component to component where research is referred back to multiple times throughout. This table acts as a path for this literature review chapter to take place in each of their respective categories.

Table 1. VRF component reference chart

Reference	Multi-Evaporator			Refrigerants									Compressor			Thermal Comfort
	Double	Triple	4+	R22	R32	R134A	R125	R290	R407C	R410A	R600	R717	Digital Scroll	Inverter Scroll	Single Speed	
[1]		X														
[2]						X			X	X						
[3]										X						
[4]					X	X	X		X					X		
[5]	X			X												
[6]														X		
[7]													X			
[8]	X													X		

Table 1. VRF component reference chart (continued)

Reference	Multi-Evaporator			Refrigerants									Compressor			Thermal Comfort	
	Double	Triple	4+	R22	R32	R134A	R125	R290	R407C	R410A	R600	R717	Digital Scroll	Inverter Scroll	Single Speed		
[9]																	X
[10]				X					X	X							
[11]			X			X		X		X	X	X					
[12]			X			X		X		X	X	X					
[13]		X												X			
[14]										X			X		X		
[15]													X				
[16]													X				
[17]	X																
[18]		X															X
[19]																	X
[20]			X										X				
[21]		X												X			
[22]			X											X			
[23]													X				
[24]		X															

Multi-Evaporator Air Conditioners

It is observed that multi-evaporator configurations generally consist of two to five for residential and more than five for commercial uses. Since VRF systems are expensive the first segment of review investigates just that as subsequent components will be resulting conditions of evaporator unit expansion. Modeling and simulation experiments are evaluated in addition to physical experiments as calculations for more than two units prove to be cumbersome for continually experimenting physically. Computer aided calculations effectively provide a preliminary position to start at for field investigations.

Dual Evaporator. A traditional HVAC split-system or single evaporator VRF system has one single input and output being target set point and system operation (on or off). A dual evaporator introduces additional inputs as temperature range from the target

set point and the alternate evaporator operation status along with additional outputs as refrigeration line pressures and temperature and air supply temperature. The output occurs after many controlling parameters are met in order to provide a specific airflow with an appropriate temperature given that the remaining components are maintained at a level of acceptable reliability. In order to test conditions of a dual evaporator configuration Shah et al. [5] investigated situations of reducing airflow in one of the evaporators in order to investigate the superheat response. Since both evaporators were running identically, when the first evaporator held a reduced airflow the superheat decreased as well as zone temperature. As a response to the first evaporator airflow reduction, the superheat measurements from the second evaporator slightly increased and a small decline in zone temperature took place. This response indicates how this type of system is fully attached to itself and how experimentation is vital in the full development of future VRF systems as the response may be different in a scenario with different sized zones. Alternative variations of this scenario will be investigated later when compressors are in discussion since the compressor was in steady state during this time.

As the development of VRF systems is still underway, test conditions have yet to be normalized and are logically in placed for pertinent resulting information. Choi and Kim [8] tested a dual evaporator VRF system where the first evaporator had a moving range of load conditions while the second evaporator maintained a specific EEV position and load condition, all the while the compressor was held at a constant speed. Total load capacity is monitored and compared between tests alongside superheat and mass flow rate. Similarly, to the results of Shah et al. [5] there are adverse effects when altering one of the evaporator units that show changes in control need to be handled appropriately to

accommodate for the variable mass flow rate and capacity that is being called in the first evaporator. Superheat is monitored while compressor speed is incrementally increased from 30Hz to 63Hz and it shows that when the air temperature at each evaporator is equal that the superheat difference between the evaporators fluctuates between 0.25°C and 2°C. Alternatively, when the air temperature at the evaporator units has a 5°C difference the superheat is less volatile and responds similarly across both units. Developing for general VRF system is slow in comparison to a specific setup as response between various configurations has yet to be generalized. Yan et al. [17] modeled a dual evaporator system that was focused primarily also on pipeline length however the end results loosely play into response results from Choi and Kim [8] and Shah et al. [5] as it was found best to locate the outdoor unit equidistance between each evaporator. The dual evaporator configuration is more common in early development phases but the push for larger configurations is growing.

Triple Evaporator. Before discussing fully expansive systems the next iteration is for a triple evaporator set up. To reiterate, a single compressor is still traditionally used with each evaporator having a respective EEV to modulate refrigeration flow rate. While Lin et al. [1] focused aspects of the paper on specifically controlling algorithms, there were some realizations and response to testing the triple evaporator set up that pertain to this review. The expansion and full control of a VRF system increases the number of output variables to dictate input parameters. The growth of input and output variables does not occur in a linear fashion with each additional evaporator. Every aspect of controlling must work in collaboration to adjust the compressor speed and each EEV however it is not a simple increase or decrease in orifice openings; the EEV adjustments

must be analytically arrived at in near real time for respective system response time. Lin et al. [1] held the evaporating temperatures (located at the exit of the evaporator) as a primary output to monitor to keep appropriate levels of superheat with correct EEV openings. The testing consisted of a triple evaporator setup with variable options in the model for direct expansion of an additional evaporator and EEV. As seen in dual evaporator configurations superheat remains volatile with multiple units handled by a single compressor with a shared refrigeration line. At the time study from Lin et al. [21], the balance of control and reliability is a fine line. The controlling range of the triple evaporator system is widened however it increases the unreliability as superheat is harder to control for each evaporator. The indoor unit fans were held at a constant speed while EEV positions were altered. When the EEV positions of individual units were adjusted the superheat collectively had increased fluctuations which is troublesome as higher superheat values mean that the system is not operating efficiently and lower superheat values mean there is possibility that the phase change in the evaporators is not always exiting the evaporators at 100% vapor. Superheat fluctuation were reduced when each EEV was maintained equally to provide a more stable range of superheat that is guaranteed a vapor and a respectable level of system efficiency.

Particular studies from Meng et al. [13] are carried out dealing with triple evaporator systems however their focus is in the heat exchanger fins and alterations to the inner components. The microchannel heat exchangers contain a level of effectiveness that is correlated to compressor performance that will be conferred in subsequent component segments.

Since the progress of VRF systems is still in development, the driving parameters vary from study to study. Yan and Deng [18] investigated controlling options for a triple evaporator system that concentrates on the response of indoor relative humidity (RH). As the experiment developed from a single to a triple evaporator setup the controlling algorithm became more rudimentary from a full variable speed system to essentially a two-stage system with high and low settings in order that humidity response was relatively acceptable. Tests transitioned from variable speed to the high-low settings which resulted in a tighter controlled range of RH for each respective indoor unit zone. While the targets were met there was room for improvement to lengthen how fast the temperature and RH falls and rises. The changes to the experiment were carried out by changing from transient to steady-state operating conditions ranging from varying indoor target temperatures, sensible and latent loads.

Yan et al. [24] experimented with a three-evaporator air conditioning system to show how the system responded as individual components operated to meet their respective zone testing parameters. Airflow was maintained throughout each test and the parameters surrounding the refrigeration and performance were collected. The EEV position was not let free to adjust, it was set at a value for each segment of testing ranging from 20% to 60% only. The compressor was maintained at a constant speed of 3960 rpm with a constant supply air temperature. There is meaning behind keeping a number of variables constant, and it strives to find how each indoor unit responds to changes of other units since they are so complexly related to one another. In the first test only one indoor unit was modified to change EEV position and air temperature in the space separately to view how indoor units 2 and 3 would respond with their constant

conditions. In the second test, indoor units 1 and 2 were changed and indoor unit 3 was held constant.

There was a correlation between the two parts of the first test. Introducing higher air temperature in indoor zone 1 steadily increased the cooling capacity for the evaporator and opening the EEV from 20% to 60% in increments also increased the cooling capacity. This seemed to be expected as more refrigerant mass flow rate increases the total capacity for that evaporator. When indoor unit 1 was altered, indoor units 2 and 3 slowly lost cooling capacity as the indoor unit was increasing from air temperature or EEV opening position. Degrees of superheat were also gathered, and as the EEV position opened there was loss in control of degrees of superheat, not by much but it was a rather low value that would begin to raise flags.

In test 2 where indoor space 1 and 2 were modified, results are showing similar trends however the sharing of refrigerant with a constant compressor speed is a limiting factor. The test starts both indoor units at 40% and indoor unit increases to 60% while indoor unit 1 decreases to 20%. As expected, the cooling capacity rises for indoor unit 2 and decreases for indoor unit 1. Alternatively, when the temperature rises for space 2 and lowers for space 1, the cooling capacity increases and decreases for each respective zone. During each of the testing periods, the unaltered indoor unit maintains initial conditions within reason to not affect the remainder of the system to create instability. This indicates how crucial the system controller is to stable operation for every component to maintain reliability.

Four+ Evaporators. VRF systems in development for more than four evaporators usually pertain to specific project and geolocation. Since physical

experimentation can be costly, most studies conclude by means of simulations and mathematical models for results. Studies were conducted on a nine-evaporator system in a hot and humid setting. Saab et al. [11] [12] further investigated the system response with a focus on system exergy since harsh environments provide a higher challenge. With exergy analysis refrigerants begin to take precedence among VRF systems that follow a differing set of guidelines outside of the United States. For testing each of evaporators, a model was created, and a different load was applied to each of the units between 1.3kW and 6.7kW. The coefficient of performance (COP) for this nine-evaporator system was dependent on how the balance of pressure produced at the compressor and refrigerant type. As compressor pressure increase from 2500 kPa to 3600 kPa, the COP of each refrigerant showed the same trend of declination of about a COP value of 2. A wide range of results values for each unit is appropriate with this large expansion of a system.

The expansive system includes a larger outdoor unit than the common residentially sized unit of 1.5- to 3-ton systems. With this comes a wider range of operation modes for the system compressor. Hu and Yang [20] investigated partial loads and midrange of compressor ranges to determine more than one type of compressor can be used which will be compared among other compressors. Zhang et al. [22] modeled four indoor evaporators that posed challenges from incorporating the equation models for each component when they are all working simultaneously to achieve various parameters. A finite volume method was used for a fin and tube heat exchanger with a spatial distribution model for simpler portions of the paper. Equations presented in ARI standards were used in predicting the compressor performance alongside the flow coefficients in the ASHRAE handbook for electronic expansion valve performance. With

having a working model of their chosen system, a validation was carried out in a test facility to monitor superheat between each of the evaporators and testing load conditions and further explore compressor mode compatibilities.

Multi-Evaporator Highlights.

- Adding evaporators increases quantity of inputs and outputs nonlinearly for proper system integration, stability, and reliability.
- Testing includes, but not limited to:
 - Airflow reduction in single zone for zone response and stability
 - Variety of load conditions per single zone for stability and response in other zones and constant load
 - Different constant loads per zone for system response through EEV controller and variable compressor speed
 - EEV position changes for response in superheat measurements with a fixed compressor speed
 - Limiting ranges of airflow and compressor speed for part load condition experimentation
- Double- and triple-evaporator HVAC systems are recommended to be targeted to investigate for future residential usage as control variables are less excessive and system is more responsive than more than four evaporators.

Refrigerants

Choice of refrigerants is not solely based on performance. Environmentally friendly and nonhazardous properties drive the development in rising refrigerants. Amarnath and Blatt [10] observed that years leading into residential VRF systems there was an array of refrigerants starting with R-22 and R-407C that eventually led to the more common R-410A. Shah et al. [5] used R-22 in the dual-evaporator system validation where pressure and superheat response were focus but refrigerant was not compared as preceding review work for the experiment was based on R-22 since it is the predecessor to R-410A. R-32 is only used in R-407C along with R-125 and R-134a in a mixture. In a study by Sencan et al. [2], R-134a was resulted to have the highest efficiency in a MATLAB modeled system for superheat and subcooling properties. The system tested on was not specifically a VRF system as compressor efficiencies were applied to the model for calculations. COP was recorded from first and second law of thermodynamics analysis with R-134a, R-407C, and R-410A. R-410A was shown that although a more recent and safer refrigerant, it held a lower efficiency rate compared to the other refrigerants. In another R-407C mixture experiment, Atas et al. [4] investigated a VRF system with three evaporators resulted in a COP minimum value of 2.24 where the study from Sencan had a range of COP from 2 to 6.5 depending on the compressor efficiency and operating temperatures. Temperature control of each unit remained similar as the EEV control was maintaining proper pressure and temperature at the exit of the evaporators.

Saab et al. [11] [12] experimented with nine-evaporators and five refrigerants; R-134a, R-290, R-410A, R-600, and R-717. The highest COP over a range of compressor

pressures comes from R717 which is 24% higher than R410A with the other refrigerants falling behind 12% to 37% lower. Using R717 (ammonia) has potential to be poisonous so R410A is chosen as there must be some position where one refrigerant is better on average with various features as ozone depleting potential, global warming potential, lifetime that all factor into choosing the correct refrigerant. The potential poisonous nature of ammonia comes in the form of concentration levels that can spike due to hardware failure of an ammonia refrigerant system. The maintenance of this type of refrigerant system is where overall costs over R-22 and R-410A are exceeded as maintenance for safety is more frequent and less suitable for residential use. Between the compressor and evaporators there is a tradeoff between COP values as for the evaporator as pressure increases the COP does as well however for the compressor the COP decreases as the pressure increases. Similar responses were shown for each refrigerant over the range of pressure where R717 has the highest COP potential but incurs environmental and health threats. For comparative purpose the COP for R-410A and R-134a were 3.9 and 3.4 respectively. The remainder of refrigerants did generally maintain a lower COP they are not used due to safety and maintenance reasons.

Tu et al. [3] charged a VRF system with 16 kg of R-410A in order to record performance data. A large amount of charge was set into this system as portions can be stored in a sub-cooler that affected to this experiment. In other systems with multiple evaporators there are multiple input variables to dictate the compressor speed, fans, EEV position but this controller checks if the unit is on then looks for change in pressures and alters compressor speed if it needs to change or completely stop. A positive component to system developed controllers is how this experiment used a pressure compensation to

keep the capacity dynamic to reflect the changes in the system. The balance of compressor speed and EEV operation remain to be the controllers of performance results. Cheung and Braun [14] investigated heating mode with different types of expansion valves for VRF systems using R-410A through a thermostatic expansion valve (TXV) or a fixed orifice with an accumulator (FXO) primarily used in single speed systems. The single speed systems were compared directly to the VRF systems. COP and efficiencies of heat production, heat transfer, degradations and second law efficiency are measured and reported for the systems each kept at 2.2kg of R410A of charge. When ambient temperatures were below target set points where the system was kept at near full capacity the COP between the VRF system and the TXV/FXO systems were within a respectable range of each other. However, when temperatures within range of partial load capacity and the VRF system began to modulate compressor speed the COP exceeded that of the TXV/FXO system by up to 2.5. As a general finding, R-410A remains a common goal of uniform residential refrigerant while new refrigerants are always being researched.

Refrigerants Highlights.

- Numerous factors affect choice of refrigerant aside from performance
 - Ozone depleting potential
 - Global warming potential
 - Refrigerant lifetime
 - Overall hazardousness
- R-717 was shown to be best performing however is known to be most hazardous and highest required maintenance

- Coefficient of performance and environmental factors place R-134a and R-410A close in contention but R-410A pressure and temperature properties appropriate for a residential a HVAC system
- R-410A is current common refrigerant over pervious R-22 due to ozone harmfulness and heat transfer potential

Compressors

Digital Scroll Compressor. These types of compressors operate at full speed which would appear counter intuitive of the types of investigations in discussion. The scroll that is orbiting another scroll is what is operating at full speed, but the compressor controller lifts the scrolls away from each other when capacity needs to be adjusted. When the scrolls are separated the work done on the refrigerant is zero thus minimal energy consumption and when capacity is required the scroll is set back in starting to increase pressure and temperature of the refrigerant to the desired discharge pressure and temperature. The variation of when the scrolls are together(closed) or separated(open) is averaged by time of operation to calculate an output ratio which was used to gather the output capacity.

In the Cheung and Braun [14] study, the ductless system that was compared to a TXV/FXO system is the proof of levels of increased efficiency when using a digital scroll compressor over a simple single stage. While there are segments of ambient temperature where COP values are relatively close the subject is of longevity of efficiency for energy consumption which over a longer period of time the VRF system ventures away from the single stage efficiency base line.

Hu and Yang [20] further proves the efficacy and potential reliability of digital scroll compressors in a multi-evaporator air-conditioning system. Integration between EEV, compressor speed and capacity output were crucial in its success. The further levels of controllability allowed for zoning options of up to five indoor units on the same scroll compressor and part-load scenarios resulting in energy consumption reduction as the range of operation in this type of system ranges from 17% to 100%. Calibration was required for the usage of single EEV usage up to four components to develop a linear regression when adding or removing controlled zones and remain under the same compressor. The response parameters in check for the test were sub-cool and superheat temperatures compared with the outdoor fan speed. Compared to the traditional variable frequency-controlled compressor this was a promising increase in existing operation range of 48% to 104%.

Multiple compressor systems hold validation in evaluating part load conditions for VRF systems however the efforts are not often seen in consumer residential production. Tu et al. [23] experimentation focuses on just that with a digital scroll compressor and single speed compressor for five indoor units. Initial results indicated that the system remained stable when the digital scroll compressor had an output ratio of 100% thus closing the valve and the scrolling produced maximum capacity. This is where the secondary compressor engages. Although the digital scroll compressor is running stable, the target pressure has yet to be reached thus enabling the standard compressor to alleviate output ratio in order that the pressure be reached while attempting to remain stable. While both systems were on, the target pressure still had issues of being reached until the output capacity was reduced. When the digital scroll compressor had a low

output ratio of 20% is when the standard compressor reverts to on-off status. Results showed where the fluctuation of supply air temperatures were from on-off cycling of the standard compressor than attempt to aid the digital scroll compressor. In efforts to improve the experiment, average suction pressures were taken during a period of on and off stages of the digital compressor to control the output capacity differently in order the target pressure has been met. The goal was met to have the pressure maintain an oscillation that was within a defined range due to an averaged suction pressure across cycle periods.

A testing methodology has been documented for VRF systems with a multi-compressor configuration as previous by Xia et al. [7]. While this methodology is for a heat recovery system, the compressor configuration response is relatable. The performance for part load conditions was exceptional as this is where both the variable speed and single speed compressor are engaged. This band of higher efficiency is where the system begins to engage the single speed compressor as where the previous investigation sought out to find the optimal frequency at which to engage the secondary compressor. Part load conditions is the beginning of increase efficiency, so it is no surprise there are numerous investigations regarding a dual-compressor configuration. Similar to previous multi-compressor studies, Zhang et al. [15] also experiments with a VRF system with a single speed compressor complementary to a digital scroll compressor to evaluate part load conditions for a four-zone system. This compressor configuration is controlled by pulse width modulation (PWM) so it was determined using COP and energy efficiency ratio (EER) is not optimal as PWM varies with time.

A simulation model was presented by Min et al. [16] using an injected scroll compressor and sub-cooler. Parameters measured and developed were degrees of superheat and sub-cool, alongside efficiency and the amount of injection ratios. Carried out for the cold seasons, an increase in injection ratio also increased efficiency of the compressor found by differences of pressures. Varying portions of mass flow rate made the same periods of injection windows longer thus making ratios higher and increasing mass flow rate from the compressor. The digital scroll compressor in different climates proves to be versatile for further development such as vapor injection.

Inverter Driven Compressor. These types of compressors similar to the digital counterpart also have scrolls orbiting however there is no moving of the scroll to disengage the compressing of refrigerant. The variable part of this compressor is a variable motor that adjusts the speed of the scroll motor thus adjusting the compressor capacity.

Atas et al. [4] evaluates a system ran by an inverter driven compressor. The compressor was initially operated at a static 50Hz with a set temperature for the system targets where the pressure between each of those scenarios were nearly identical to each other indicating good reliability throughout a cooling mode range of set points. The PLC (programmable logic controller) introduces variable speed to the compressor that is calculated from input temperature throughout the system response. Remainder of results were comparison between static 50Hz compressor speed and variable compressor speed. Overall the PLC method maintained a lower energy consumption rate. The notable point when comparing the COP to the energy consumption is that when the compressor speed is held at a static 50Hz, the COP is lowest at 2.24. This does not automatically dictate that

single speed compressors are superior; it just remains that for this speed and configuration for testing shows that single speed systems do have their place. The PLC method locates the balance of energy consumption with wanting to keep the COP higher. The actual temperature control is similar between both methods.

Lin et al. [21] experiment contains a 0 to 100Hz inverter driven compressor alongside a 480-step EEV. Feedback control loops are discussed for control but not heavily considered for this review paper. Alongside the control loops, EEV control was also discussed as theories are presented in order to control the flow throughout the evaporator and EEV positioning effects on temperature parameters. Lin experiments and models the system as all evaporators are active each requiring EEV control for capacity. Typical situations where various zones may require different capacities to reach their respective temperature settings rather than all constant values throughout. It was considered that each zone is on and demanding respective refrigerant flow. Variation of targeted evaporator temperatures proved that different evaporators can be controlled by this logic of flow distribution. In development of multiple (more than two) evaporators the control development can be extrapolated to conform to as many evaporator units as needed. The effectiveness of this particular control is currently limited to the entire system being completely on and simplifying EEV modulation of refrigerant flow distribution.

Zhang et al. [22] studied finding an alternative or competitive system to variable speed compressor systems posed many challenges as variations needed to be validated. Where inverter driven compressors generally include a variable frequency drive to control the motor speed from frequency and voltage, a rapid cycling compressor is relied

upon cycling period variations. One cycle period in a rapid cycling compressor consists of a load and idle portion. The amount of time spend under load is affected by the system determined duty ratio. Going into this study, concerns were held regarding the idling portion of the cycle period where there is no compression during idle phase and a designated amount of power consumption for the idling motor function to fill the duty ratio and complete the cycling period. Introducing partial loads to compressors truly tests the reliability and efficiency of a compressor as some may indicated higher efficiency but only at higher loads. Parameters of cycle periods indicated that change in cycle period time will not affect the overall performance. The coefficient of performance only shows slight differentiation when the cycle period is at its lengthiest time frame. Benefit of a rapid cycling compressor over an inverter driven compressor for a VRF system has yet to be seen.

Choi and Kim [8] tested variations between the two indoor units was a 21°C (70°F) and 27°C (81°F) for indoor unit 1 and 2 respectively. At a testing condition of constant compressor speed the primary source of cooling capacity is focused into indoor unit 1 at lower temperature conditions of 21°C (70°F). Variations of keeping EEVs separately constant and or controlled is tested alongside changes in compressor speeds that ultimately grant a maximum cooling capacity overall when the superheat is maintained at 4°C. Superheat without control continued to rise as there was a segment of the experimentation where the EEV was maintained at constant opening where the alternate indoor unit was controlled and the superheat was between 4°C – 10°C. Subcooling was kept also between 4°C – 7°C. Meng et al. [13] experiments with a three evaporator system with an inverter driven compressor and additional solenoid valves to

increase system pressure during start up periods. There is an oil management phase where if the compressor runs below a designated speed (35Hz) for longer than 60 minutes then a valve opens to introduce more oil to the compressor to improve longevity. Without safety measures, failure would be imminent for a system that can run for extended hours. The remainder of the investigation included focus on a developmental type of condenser under part load conditions ranging from 20% to 120%. The trends found between condenser modifications were minimally different.

Tu et al. [6] continued to investigate a multi-compressor arrangement consisting of an inverter driven compressor and a single stage compressor. The goal of this was to create a larger band of efficiency while using both compressors to achieve a higher demand while maintaining acceptable noise levels. At a certain compressor speed the frequency of the driver will engage the single stage compressor to aid the inverter driven compressor. Determining the point at which the secondary compressor engages is crucial to ensuring stability and system performance. Field experimentation showed that in the midrange efficiency performance was high while the outer bands of operation showed poor levels of efficiency with an increase in noise levels at the higher band. The multi-compressor has potential but not specifically a direct need within VRF development.

Single Speed. For a number of studies regarding improved efficiencies and performance, results are often compared to that of a single unit split system that has a single speed compressor. However, from the variable speed compressors discussion it is not uncommon for a test to operate a variable speed compressor at a constant speed in order to test other response and variables throughout the system. The study by Cheung and Braun [14] included the TXV/FXO based expansion system containing the data from

testing two different types of single speed compressor configurations against an EEV based variable speed compressor system. This data shows where variable speed compressor excels and where the single speed compressors are similar in COP. The inclusion of single speed compressors to variable speed compressors to make a multi-compressor system is worth the time spent on the research however the cost effectiveness is less than a single variable speed compressor for the VRF system.

Compressor Highlights.

- Digital scroll compressors run at full speed uninterruptedly with a mechanical part that separates top and bottom of the scroll compressor to reduce work to zero and create no pressure difference
- Inverter driven compressor, while similar to the scrolling compressor principle, contains a motor that adjusts the speed of the scrolling action to appropriate temperature and pressure control for partial load conditions; no top and bottom separation
- Multiple compressor systems contain a variable speed and a single speed compressor that achieved higher COP values
 - While max load conditions are met with both compressors, the variable speed compressor begins to decrease with respect to declining ambient temperatures in later portion of a day
 - COP values are averaged over a shorter time span with two-compressors show increase over single compressor systems in early phases of VRF development

- Inverter driven compressor variability allows for testing in stages of a fixed speed to evaluate the remainder of system components then adjust to a higher or lower speed and analyze
- Testing between the studied systems show variation in results and system response as each control is particular to that system reliability
- Future investigations should continue with partial load conditions utilizing only one compressor with at least two evaporators in efforts to generalize a controlling application and guidelines for a residential system

Thermal Comfort

Proper thermal comfort does not rely solely on target temperatures but relative humidity as well. System testing for controlling sensitivity is necessary in order that zone temperature is steadily reached opposed to immediate cooling that leads to consumer discomfort or noise issues from having too fast of air flow speed. Yan and Deng [18] developed a controlling method for a triple evaporator system based on previous research regarding a single and double evaporator system. The leading information that drove this study held a temperature-based control for one system and a humidity-based control for another system. Yan and Deng [18] integrated these systems to simulate overall response in both temperature and humidity means. The initial experiment consisted of each of the three indoor units' target temperature set to 26°C (79°F) with an outdoor ambient temperature of 35°C (95°F). The sensible load varied between the indoor units from 1150 W to 1350 W and the latent load varied from 450 W to 650 W. The results showed that the variation of sensible and latent loads affected only the patterns of response of temperature and RH while maintaining good control of the system within range of the

target temperatures. The first indoor unit had the lowest sensible and latent loads at 1150 W and 450 W, respectively. This showed where the lower bound of temperature control was reached prior to the other two indoor units and by this happening their controller reduced air flow and refrigerant flow was reduced. Yan and Deng [18] carried out a second test that put each unit's target temperature within 1°C (approximately 1.9°F) of each other with indoor unit 1 at 27°C (80.7°F), indoor unit 2 at 26°C (78.8°F), and indoor unit 3 at 25°C (77°F). Sensible and latent loads are held constant throughout each component at 1300 W and 500 W. The test variation happens at 40 minutes where the indoor unit 1 is altered from 1300 W to 1400 W sensible load and 500 W to 700 W latent load. The results showed that the change in load increased the relative humidity by 3% while maintaining target temperature at 27°C (80.7°F) in a looser pattern of modulation. The response time for zone 1 was approximately 30 minutes for the zone temperature and zone RH to reach a steady level. The other two zones were hardly affected and showed no noticeable response.

Park et al. [19] experimented with EnergyPlus simulations to compare to configurations of a VRF system with and without outdoor ventilation. This study stretches the limit of this review that investigates into ventilation contribution however needs to be addressed in efforts to convey the importance of possible humidity control for future usage. Using ASHRAE thermal comfort standards Park et al. [19] found that for this non-residential building with a VRF system without any ventilation grants less than 20% acceptable comfortable conditions for winter and summer seasons. The addition of any ventilation, whether it be an energy recovery ventilation (ERV) or a dedicated outdoor air system (DOAS), moves ASHRAE acceptable comfortable conditions in the

winter and summer season in the range of 65% to 94%. This goes to justify the system response from Yan and Deng [18] for the triple evaporator configuration with adjusted target temperatures and reduced humidity response from load changes in order to maintain a level of thermal comfort that is acceptable. Alahmer and Alsaqoor [9] simulated a multi-level building with multiple split systems throughout each level but investigated thermal comfort for a room during summertime that further responded to Yan and Deng [18] that efforts are to be made that as temperature rises in the zone, the relative humidity should be reduced in order to remain within acceptable comfort ranges.

Thermal Comfort Highlights.

- After general system response with stability and reliability is achieved, controlling methods are investigated with thermal comfort in consideration
- Relative humidity held a focal point for a specific triple evaporator configuration that showed moderate speed and steady RH fluctuation with sensible and latent load adjustments
 - Measurement of thermal comfort comes with several qualifications and standards to follow that will need to be followed more closely after multi evaporator systems become more common
- More common systems will introduce ventilation variables that were shown to drastically increase thermal comfort based upon ASHRAE standard

Chapter 3

Materials and Methods

Research Facility

The research house of relevance in this study is a conventionally design home with energy efficient features that grants a home energy rating system (HERS) index of 65 where standard new and existing homes index at 100 and over. An HVAC system has been fit in the house, with the aforementioned VRF configuration, by Trane that will cater to zoned air conditioning during a summer season. Appendix A showcases site images of the research house on the right and the respective technical floor plan. Following sections will show the potential for ductless and ducted zones and how regions were planned for sensor placement.

Layout and Zoning. In this study, the zones were divided through the research house for ducted zones and ductless zones. Existing ductwork was modified to negate airflow to the dedicated ductless airflow zones. Figure 2 shows the supply and return ductwork for the air handler unit (AHU) located in the attic and highlights where the highwall units are located. Largely zoned, the ducted zones consist of the bedrooms on the west side while the highwall units (HW) are in a shared zone of the kitchen and living area. A third HW is placed in the garage to dedicate a constant load to the system. This house is not occupied and has minimal furnishings that provide suitable working space, so thermal load is vastly from heat gain during the summer season.

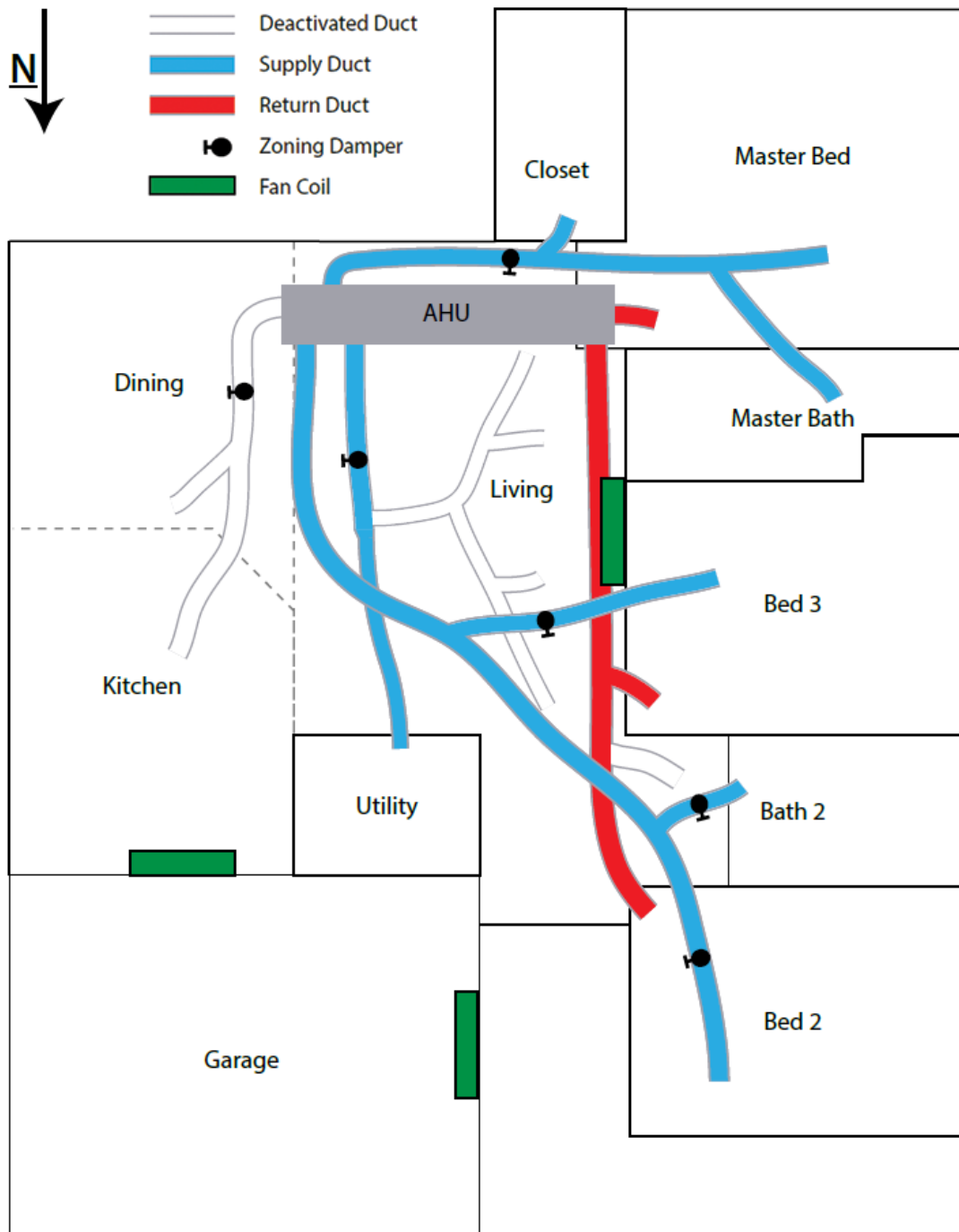


Figure 2. Ductwork and HW layout

Measurement Locations. This section pertains only to air temperature and relative humidity measurements. For this specific configuration there was not a standard or methodology to follow directly, so extrapolating information from standards and protocols were necessary to appropriately acquire data. Table 2 shows information taken from ASHRAE Standard 55 – Thermal Environmental Conditions for Human Occupancy [25] and ASHRAE Standard 113 – Method of Testing Room Air Diffusion. [26] Horizontal orientation was addressed first since ducted and ductless zones were already determined.

Table 2. Location planning for data acquisition

ASHRAE Standard	No. Positions	Horizontal	Vertical (in)		Test Points
113	4 @ 2 ft-6 ft apart	>2ft from wall or obstruction	4		4, each at vertical distance above floor
			24		
			43		
			67		
55	Up to 5	Center of Room, 3.3 ft from center of each wall	Sit	Stand	3, each at vertical distance above floor
			4	4	
			24		
			43	43	
		67			

Figure 3 shows the zones that are relevant in the lightest green color and representing the horizontal limitations from ASHRAE Standard 55 and 113 are shown in darker green areas. To incorporate the two standards one testing zone is based on the 2 feet from any wall requirement and an additional center zone (darkest green) is based from the 3.3 feet from each wall requirement. Noticeably, the HWs and air registers have a level of air distribution centricity to the planned location zones. This layout will serve as a map when sensors are ready to be placed throughout each zone.

Vertically there are commonalities between the two standards at 3, 24, 43, and 67 inches from the floor. Between a total vertical stratification, sitting, and standing, 43 inches was the height agreed upon to have temperature and RH sensors located. These sensors are stationary throughout the seasonal experiment. Interests in spatial relationships led to installing two additional systems; a mobile pole with thermocouples at each of the standardized measuring points for vertical stratification and a wall mounted thermocouple grid for spatial relationships for thermostat or controller placement.



Figure 3. Spatial location planning for sensors

Sensors

Choosing the proper sensor is vital in research due to many requirements for performance and accuracy of the sensors' input and output. Similar to positioning of the measurement areas, information on requirements and guidelines had to be extrapolated from reliable standards and protocols.

Selection Process. In addition to ASHRAE Standard 55 and 113, Standard 70 – Method of Testing the Performance of Air Outlets and Inlets [27] was added for information regarding accuracy requirements for temperature and RH. Table 3 shows the ASHRAE accuracy requirements for air temperature, RH, and air speed along with relevant requirements from the National Renewable Energy Lab (NREL) [28] protocol for mini-split heat pumps.

Table 3. Accuracy Requirements

Variable	ASHRAE Reference	ASHRAE Accuracy	NREL Accuracy
Air Temperature	Std. 55 - 7.3.4	±0.4°F (±0.2°C)	
	Std. 70 - 4.1.1	±0.2°F (±0.1°C)	±1.1°F (±0.6°C)
	Std. 113 - 5.1,5.2	±0.4°F (±0.2°C)	
R. Humidity	Std. 55 - 7.3.4	±5% RH	±3% RH
Air Speed	Std. 55 - 7.3.4	±0.05 m/s	

An acceptable range for air temperature sensor accuracy is from ±0.2°F to ±1.1°F and an acceptable range for humidity is from ±3% to ±5% RH. The range of accuracy for RH is from 25% to 95% so this is acceptable since research sites' daily average humidity is

soundly in the range. Air speed sensor accuracy should be ± 0.05 m/s (± 10 fpm) while not exceeding 0.15 m/s in speed.

Temperature measurements were agreed to be taken from T-type thermocouples. The range of accuracy was at the limit of the requirements, but plans were made to calibrate thermocouples by means of ice bath and boiling water to eliminate outliers and compensate prior to full data acquisition. Relative humidity sensors were not required to be at every position there was a thermocouple but only in each respective zone. Sensor count came to be 42 temperature measurements and 8 humidity measurements for zone and spatial relationships. The choice of sensor for RH was a Dwyer RHP-2W10 that had a 2% RH accuracy and operated on a 4-20 mA output signal. Both the thermocouples and RH sensors were wired to National Instruments hardware that will be discussed in a subsequent section.

Installation. From the measurement areas planned previously, Figure 4 shows where thermocouples (blue) are placed with one RH sensors (magenta) in each zone. Having a large quantity of spatial thermocouple positions created potential issues with running wire across the floor and also having to construct a way to hold each individual thermocouple. It was cleaner and inexpensive to let the thermocouples hang from the ceiling. Previous projects had wiring paths installed that allow wire management throughout the attic area and down into a maintenance room that housed data acquisition hardware. Nearing the end of wire installation, it was found that there was a mixture of J- and T-type thermocouples. Reluctant to continue, software management fixed any type of discrepancy. The thermocouples were arc welded together and fed through acrylic tubing to keep them straight and manageable. Figure 5 shows the living room area with installed

thermocouples and RH sensors. Appendix B contains images of full installation in each zone as well as the auxiliary temperature measurement systems on a vertical pole and wall mounted temperature grid in Figure B7 and Figure B8, respectively. Additionally, there were thermocouples installed at the air register in each of the ducted zones to measure difference between supply of the AHU and the supply to the zone to give the notion of the heat gained through the duct work in the attic.

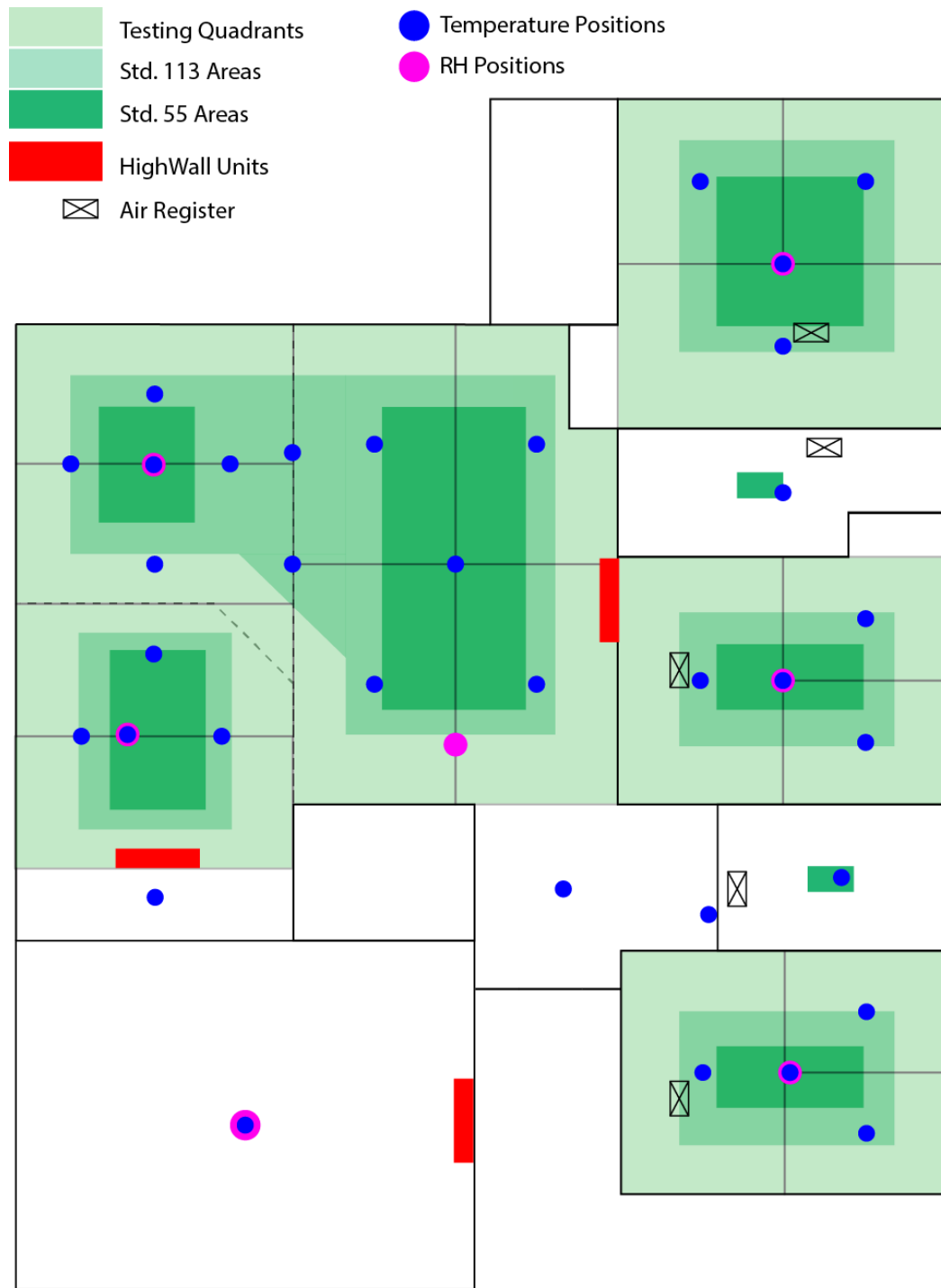


Figure 4. Thermocouple and RH sensor positions



Figure 5. Living room with hanging sensors

Installed Hardware and Components

Upon introduction to this project, the following VRF HVAC components were previously installed and undergoing initial operating strategies. When Trane personnel installed the components system sensors were also wired and connected. These system sensors are independent to that of the previously discussed thermocouple and RH sensors. This section will cover what VRF HVAC components are on site and which system sensors were operational.

Outdoor Unit. A 3-ton outdoor unit consisting of an inverter driven scroll compressor, condenser and fan is working for the entirety of indoor components. Figure 6 shows its installation position on the west side of the research house.



Figure 6. 3-ton outdoor unit

Figure 7 shows the refrigerant pipe sight glasses that were installed in line for the suction line returning vapor to the compressor and the liquid line delivering liquid to the indoor evaporators. This proved beneficial when testing errors occurred to check the sight glasses to verify there was only vapor in the suction line. If there was bubbling then there was a portion of the refrigerant entering the compressor that was liquid, so testing conditions were reverted and adjusted.



Figure 7. ODU refrigerant line sight glass

ODU System Sensors. The ODU had measurements taken from entering the compressor to exiting the condenser. There are spare measurements that are not vital to research and analysis, but the relevant ODU system variables are listed:

- Compressor Speed
- Suction pressure
- Gas temperature
- Saturated suction temperature
- Superheat
- Liquid temperature
- Liquid pressure
- Saturated liquid temperature
- Liquid sub-cool

Indoor Units. Figure 8 shows the collective zones of kitchen, dining area, and living area for the ductless zones (excluding the garage). Seen in the background are the two highwall units located in the kitchen and the living room. All-inclusive in each HW unit is the evaporator coil, air flow fan, and EEV. Upon installation the HW unit internals (control panel) were placed outside the unit for easier access to upload software changes. For refrigeration flow, each EEV has a position range from 0 steps (closed) to 500 steps (full open). HW unit fans are controlled by pulse width modulation (PWM) that creates a range of airflow operation up to 400 CFM. This was verified by connecting The Energy Conservatory's Minneapolis Duct Blaster system, shown in Figure and Figure, with each of the provided airflow rings that allowed for proper pressure differential measurement within the air flow measurement system.



Figure 8. Kitchen and living room highwall unit positions

For the front, middle and master bedroom, Figure 9 shows the AHU and ductwork leading to the bedrooms. With being a conventionally designed home, this attic can reach 120°F during the hottest part of a summer day. Similar to the HW units, the internals of this AHU are set aside for easy software changes. Atop the AHU is the refrigeration pipeline manifold, Figure 10, where refrigerant flow from the ODU is divided among the four indoor destinations.



Figure 9. Air handler and ductwork in attic



Figure 10. Refrigeration pipe manifold

Indoor system sensors. Each of the HW units are measured identically and the AHU contains extra measurement points as the ductwork allows for proper measurement of supply and return air. The list of sensors below will indicate measurements specific to the AHU, otherwise each of the four indoor units contain the same measurement.

- Superheat
- Zone temperature (Master room for AHU)
- Airflow CFM
- EEV position
- Gas temperature
- Liquid temperature
- Demand capacity
- Zone temperature set point

Demand capacities are calculated through the controlling algorithm that commands airflow and EEV position to ensure phase change through the evaporator to get proper exit measurements. For all of the system sensors and variables, data is reported to an online database for storage and access through other software means that was set up by Trane personnel.

Data Acquisition

Existing projects and installations left National Instruments hardware readily available for use. The CompactRIO (cRIO) controller accepted a wide range of modules for data acquisition, so this section will cover the components used with the CompactRIO controller.

Hardware. The diverse capabilities of the cRIO controller allows for the data acquisition of multiple different variables simultaneously with the correct cRIO modules appropriate to the data type. Using an analog current loop of 4-20mA, which is the standard for industrial instrumentation [29], grants a larger range of transmitted data.

Aside from the range, the rejection of electrical noise is a plus for data acquisition which is where voltage connections could pose issues at longer wire lengths. A referenced single ended configuration was the desired type of current cRIO modules that allowed for more inputs. Measuring voltage through an RSE terminal would place limitations to have a wire length of less than 10 feet if the signal is over 1 V, which it was. The selection was a NI-9208 16-channel RSE ± 20 mA current input module. Thermocouple cRIO modules involved less decision making as there were some existing NI-9213 modules already in use that just need some adjusting for free space. An existing NI-9201 voltage input module was still active for auxiliary temperature and RH measurements inside the AHU ductwork. Images of the National Instruments hardware can be seen in Appendix C. A separate cRIO handled the two auxiliary measurement devices that was manually accessed when data was required at specific positions throughout a zone.

LabVIEW Virtual Instruments. The micro-processing power of the cRIO system allowed all fifty signals to be placed into a single virtual instrument (VI) without time loss. There were two VIs that are programmed to handle all of the acquisition and forwarding of data. In the acquisition sub-VI, each signal was acquired and indexed then taken a running average of per 15 seconds. Each value was fit into a cluster type data set that was then passed on to a separate VI. The sub-VI used is shown in Figure 11 and the main VI is shown in Figure C3. The main VI is calling for the data set created by the sub-VI to flatten to a string and send to an online database via TCP/IP protocol.

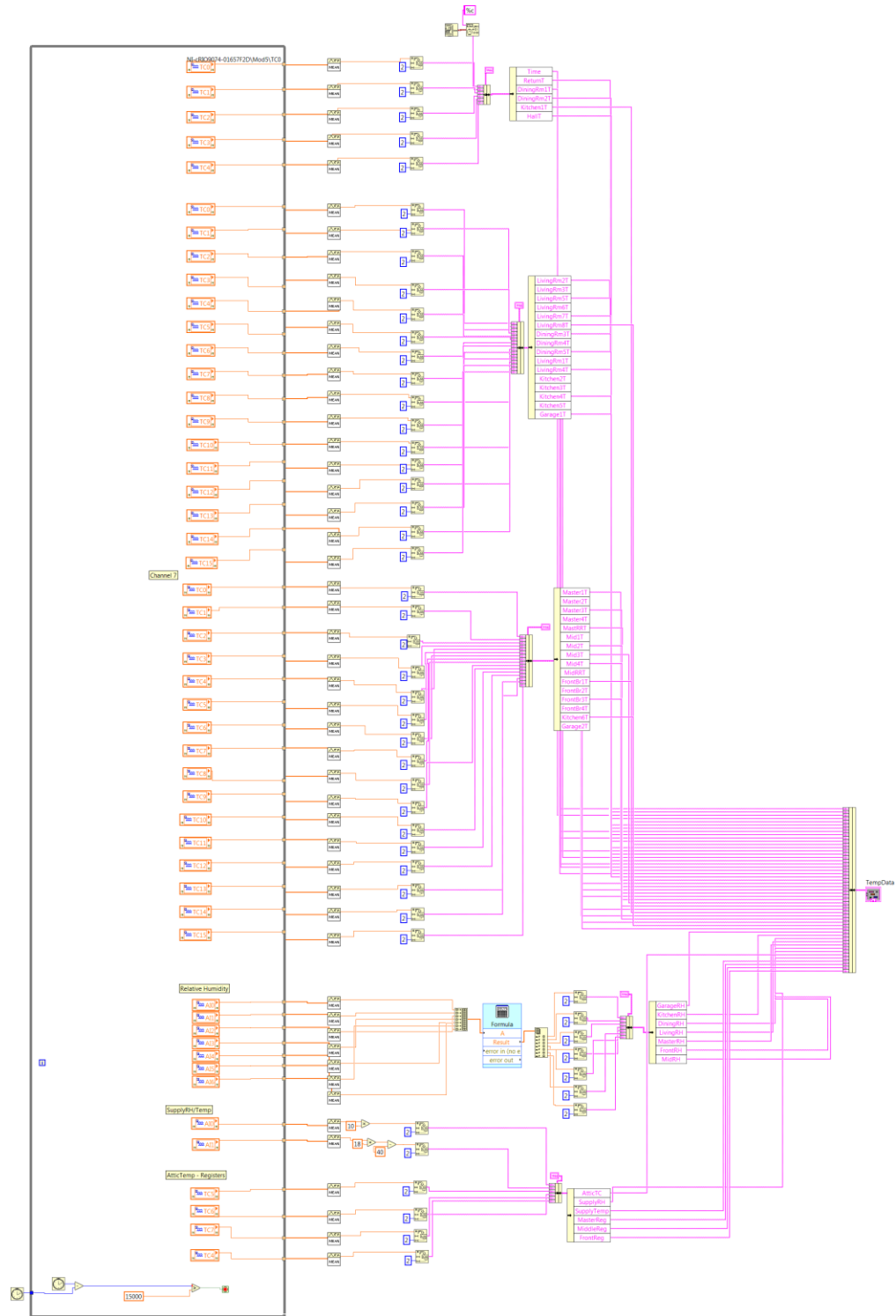


Figure 11. Sensors signal acquisition

Data Access. With a 15-second interval per data entry there are 5,760 data points per day. This amount of data entries per signal, both through system and cRIO, is strenuous on normal spreadsheet software. This necessitates usage of additional resources for mass data management. Using python to access a MySQL address allows for far easier data manipulation and organization.

Testing

Introductory testing methods were derived off zone control and response by applying target set points for each zone based on location and timing. Table 4 lists out scenarios for testing the hybrid VRF HVAC system. The prime (‘) indicates a modification to the original testing scenario in order to see if zone responsiveness is reciprocated. As general system stability was in place prior to project start, these scenarios for testing will validate the stability remains unbroken.

Table 4. Cooling mode testing scenario with zone target set points (SP)

Scenario	Main (°F)	HW1 (°F)	HW2 (°F)	HW3 (°F)
A	75	75	75	75
A'	Same SP, add ceiling fan			
B	75	75	75	70
C	80	80	80	70
D	72	78	78	75
E	70	80	80	75
F	75	75 → 70	75	75
G	76	74	74	72
H	75	73	73	74

Testing scenarios generally last 24 hours with a selection of 48-hour samples. For ease of application of the tests' parameters, the time window is decided to start at 10PM the evening before the date decided. For scenario A', the modification lies in turning on

the ceiling fan to observe vertical stratification of air temperature. scenario B places one zone at a different set point by 5°F. scenario C places a one zone at a different set point by 10°F. Scenario D places each zone within 3°F of each other between 72°F and 78°F. Scenario E placed each zone within 5°F of one another and scenario F changes set point midday by 5°F. After observing results from other tests, scenarios G and H were derived for a closer look at zone response since the kitchen and dining room areas are not exclusive to their own space.

Garage measurements are taken and monitored however, the purpose of having a HW unit in the garage is to synthesize a load on the system. There is a minimum the system requires to be on which may not be met naturally due to the house being unoccupied, so a constant load through the garage is where it comes from. Set point temperatures in the garage are designed where they are going to generally be met during evening time and to keep striving against ambient heat gain during midday.

Chapter 4

Results and Discussion

With many variables present in the hybrid VRF HVAC system and also throughout the research facility, a general outline of relevant variables was planned and programmed via python scripting to populate the graphs when a day of data was required. Table 5 shows the eight general resulting data output plots. Compressor speed was measured in revolutions per second (rps) and all temperatures measure in Fahrenheit. Superheat measurements are shown as the amount of degrees above the refrigerants' current boiling point (saturation temperature), not the actual temperature of refrigerant in line. The line pressures and temperatures are from the suction line and liquid line, located at the entrance of the compressor and exit of the condenser respectively. The system states are the operating state the system is going through at that time. The primary system operation states of concern are 'cool joining' where a HW unit or the AHU is activated, and 'cool leaving' where a HW unit or the AHU is deactivated. The other states are when the entire system shuts down, or the system is running based on demand capacity and no activations or deactivations of indoor units are called for. There are auxiliary plots that are specifically tailored for each test if it deems appropriate. These auxiliary plots consist of the secondary data acquisition sensors mounted on the wall under HW1 (in living room) and the vertical temperature stratification pole that can be moved around zones. Scenario A will contain each of the output plots and subsequent scenarios will have important data with comprehensive sets in Appendix D. Trends and findings through

each scenario may have required specific data output in order to find relations between two variables not specifically mentioned in Table 5.

Table 5. General resulting data output plots

Output Plot	Variables
1	Compressor speed (rps) Outdoor temperature Indoor temperature
2	Zone average temperatures Compressor speed (rps)
3	Ductless (HW) temperatures
4	Ducted (AHU) temperatures
5	Relative humidity (%)
6	Demand capacity (BTU) Zone average temperatures
7	Compressor speed Superheat
8	System state Line pressures (psi) Line temperatures

Results presented are from the 2018 summer season. Scenario A with identical zone set points was designed to be the reference day of data. The data for this day is under normal weather conditions for a summer day. Throughout days of operation data was frequently checked and there were days where system failure had occurred due to high or low pressures safety measures or obscure software errors. At this point specific Trane personnel was contacted and reported snippets of data around the failure time and possible reasons; this daily data was marked as an invalid day. Each scenario resultant will be presented and discussed for independent clarity and organization.

Scenario A.

- All zones at the same set point.
- Target set points: Main = 75°F, HW1 = 75°F, HW2 = 75°F, HW3 = 75°F
- Auxiliary measurements included for ceiling fan on and off airflow distribution.

Figure 12 is the overall performance where the compressor data trend indicates a good days' worth of data for further analysis. As a standard in result comparison and test development, **scenario A** was held as a reference with Figure 12 as a standard of acceptable condition and compressor operation. This standard of acceptable conditions was determined by Trane for their system to modulate and cycle throughout the evening time leading where heat load on the house was minimal and required minimum compressor speeds. As outdoor temperature rises, the heat load in the house requires the compressor to cycle less and less until it is continuously running and ramping up in speed.

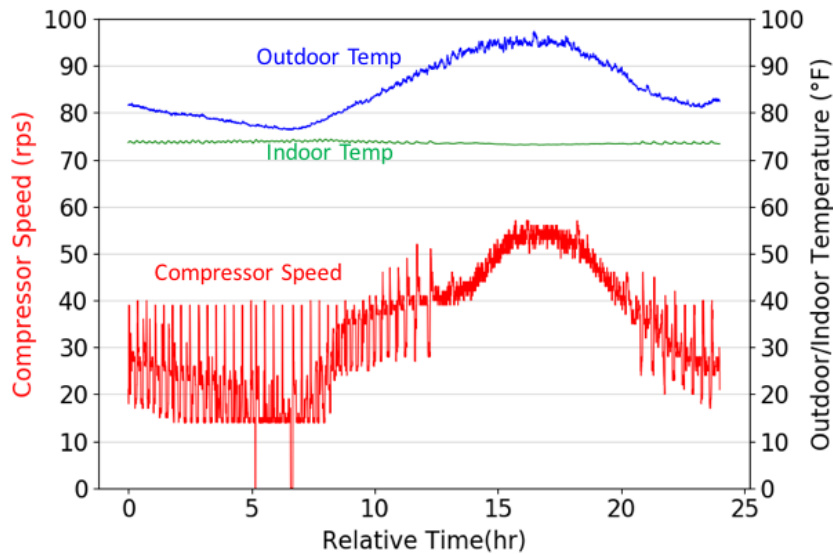


Figure 12. Normal daily data performance (Scn. A)

Compressor speed holds a key place since it mimics demand from ambient temperature that the zones are calling for, so it is seen again in Figure 13 along with the averaged

zone temperatures. These averages are of each individual thermocouple in each zone. As the floor plan has HW1 and HW3 in an open floor plan it is expected to see the zones averages close. Outliers are the middle room and front bedroom since those zones are not specifically controlled but the consequence of the master bedroom controlling temperature. While a specific spatial position was not generally considered, there are positions in the research house that affected average zone temperatures more than others.

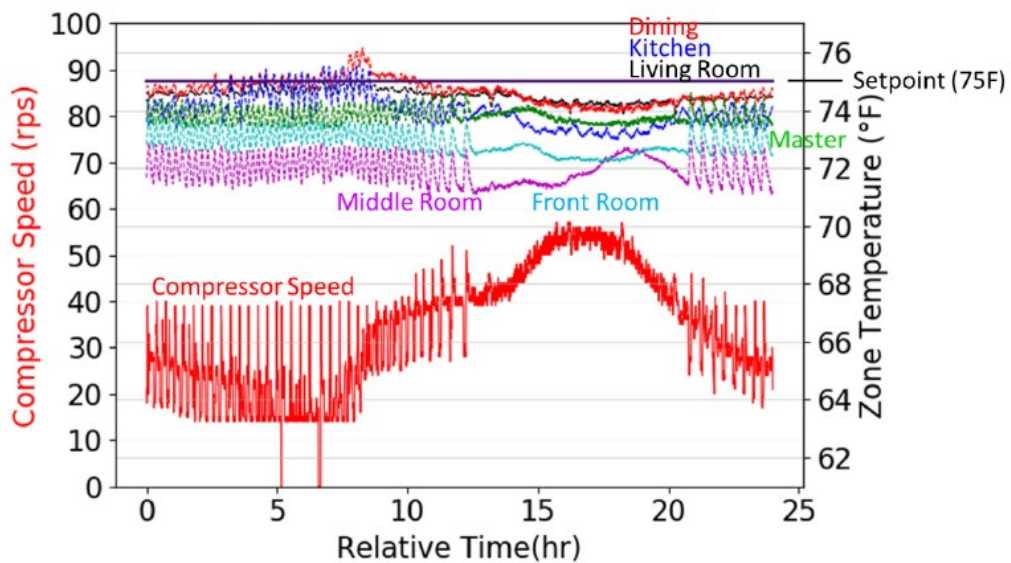


Figure 13. Compressor speed and zone temperatures (Scn. A)

As this is during the summer season, the outdoor temperature in blue declines overnight (as test started) and increased to the hottest part of the day around the 16th hour of testing which was around 3 pm in the afternoon. The indoor temperature (green line) was maintained around the 75°F target set point but noticeable it was smoother control when the compressor speed trend began to increase just before midday. If data output was not relatable to this then it was considered a poor day of data.

Figure 14 shows temperature response throughout the ductless zones (excluding the garage) totaling 17 spatial measurements along with the controlling temperature of HW1 and HW3 in the living room and kitchen areas. HW1 and HW3 temperature that are on the plot are of the controlling measurements, when the temperature falls below target the demand is calculated, adjusted then requested by the system to the compressor. In the living room temperature trends are consistent with each other within 1°F of the control measurement. The outliers in the dining room, although no HW unit, comes from HW1 in the kitchen that is lined up with certain thermocouples that are receiving direct airflow.

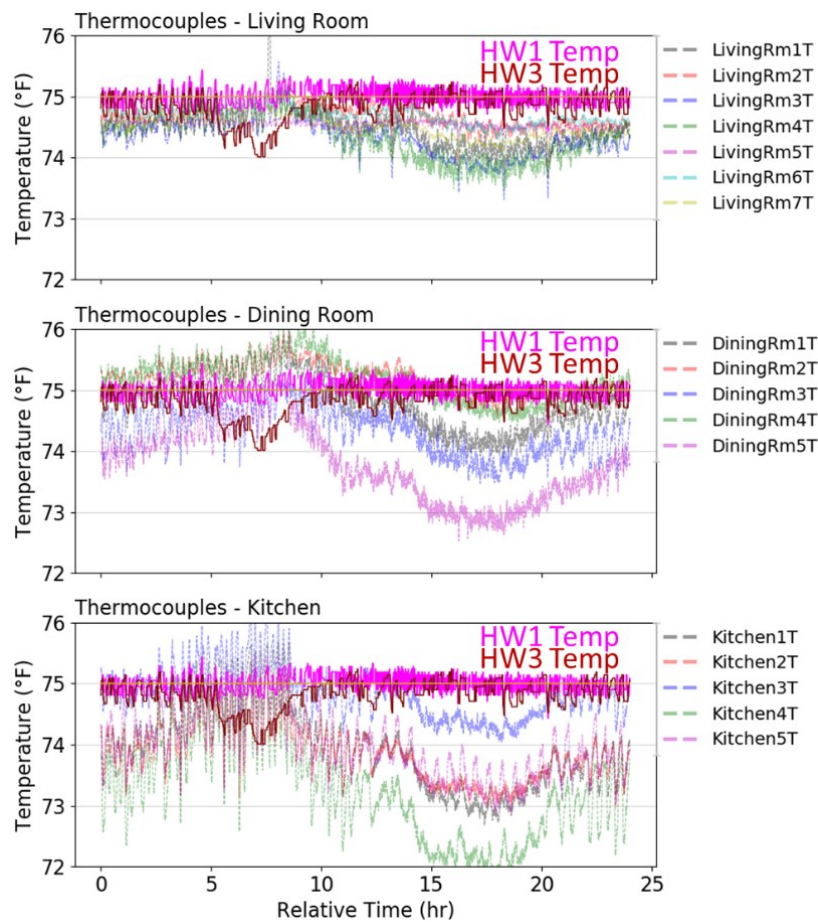


Figure 14. Ductless (HW) temperatures (Scn. A)

Figure 15 shows the ducted zones temperature supplied by the attic AHU. The front and middle bedroom are ultimately consequent of the master bedroom temperature control as the controlling sensor (thermostat in some cases) is located in the master bedroom. The main control temperature in the master bedroom of Figure 15 controls concisely during high demand times (where control is smooth and less modulated) but is led to believe contains error in measurement due to higher reading that the zone thermocouples however, changing the control temperature remain out of reach as it was previously installed and already in use.

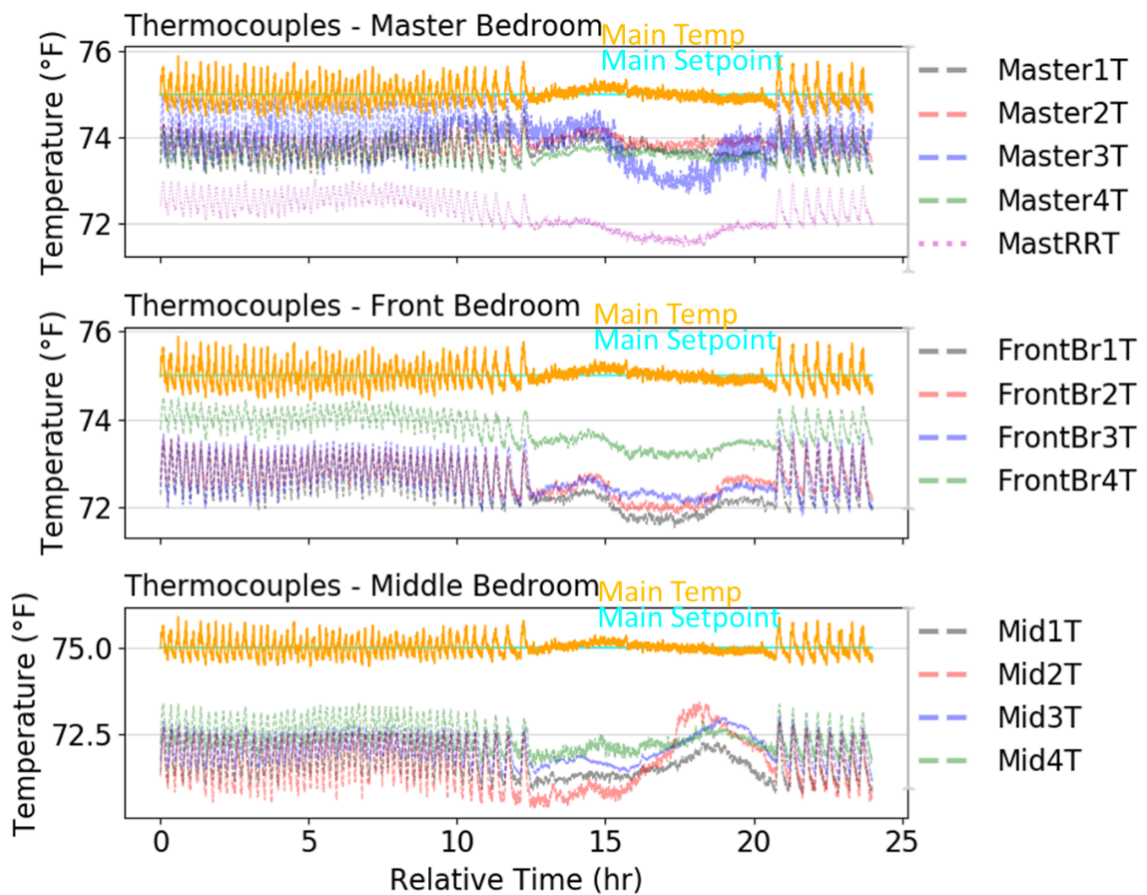


Figure 15. Ducted (AHU) temperatures (Scn. A)

The front and middle bedrooms read greater than 1°F unlike the master bedroom and were adjusted slightly by the use of in place duct dampening systems. The duct dampeners were closed by about 25% to further bring air temperature at 43” height to match closer to the master bedroom control temperature.

Figure 16 shows each zones’ relative humidity and the average dewpoint (for this first scenario). Similar to other plots garage is not reported when it comes to thermal comfort variables but only system response information. The relative humidity of each indoor zone and this is taken into account for general comfort because operative temperature is not measured and is a primary variable for thermal comfort calculations based on ASHRAE standards.

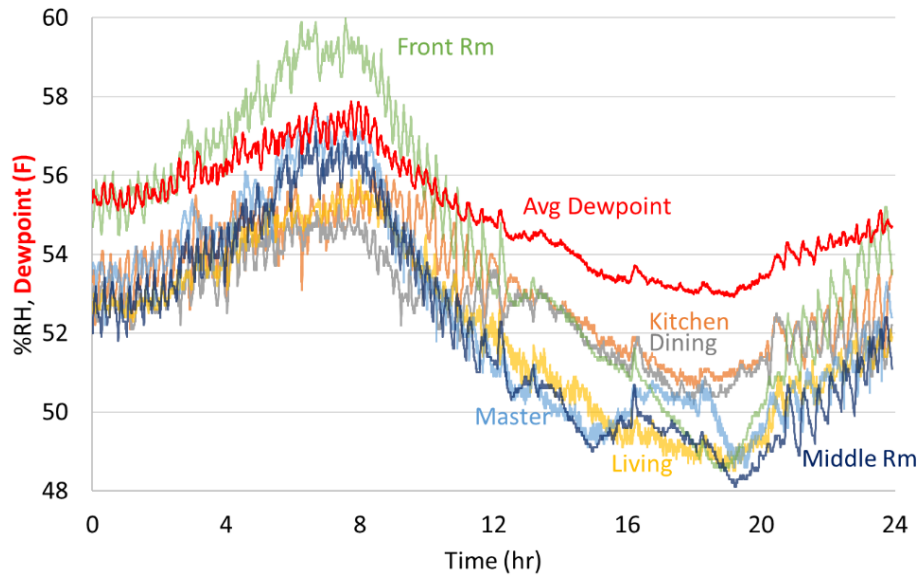


Figure 16. Relative humidity (Scn. A)

However, with knowing the relative humidity it can be estimated as the humidity ratio moves vertically on the psychrometric chart and most likely remain in compliance range

if does not fall below 40% RH. With temperature remaining controlled well around 75°F the affecting factor in comfortability is the dewpoint that rises approximately 5°F overnight creating opportunity for less comfortable scenarios if set points were closer to 70°F instead of 75°F.

Figure 17 shows the zone average temperature response to the demand capacity. System total demand is the summation of all indoor unit demand capacity requirements. As a 3-ton system, the maximum is 36,000 BTU however due to ambient temperature being so high the max is near 32,000 BTU at this time. Demand remains maxed for the HW2 in the garage while the HW1 and Main (AHU) increase and maintain targeted conditions indoor. HW3 in the living room sparingly turns on as the control temperature from previous incurred measurements that place it below the set point, so this portion of the system seen it as satisfied.

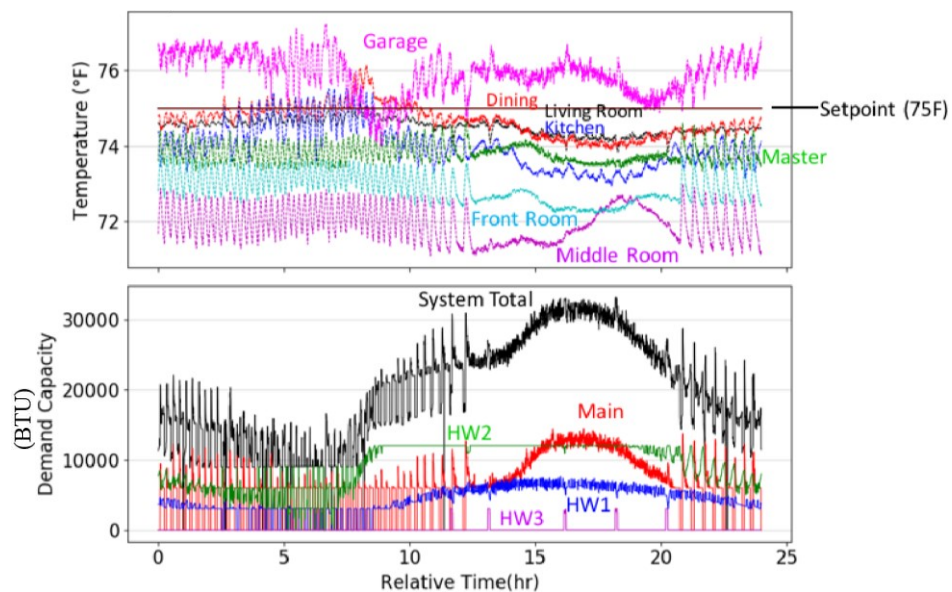


Figure 17. Demand capacity and zone temperatures (Scn. A)

When an indoor unit is not in use the superheat measurement rises through heat transfer of refrigerant as it is just sitting in the line since the EEV is closed when no demand is required.

Figure 18 shows the responsive superheat measurements and compressor activity. It is seen that HW3 is off and when it is called to turn on the superheat is immediately within an acceptable range until it is turned off again. For safety measures, the ODU superheat measurement is taken just before the refrigerant enters the compressor to ensure it is at an acceptable range. If the ODU superheat is zero, then refrigerant is entering in a mixed state of liquid and vapor potentially causing harm to the compressor internals. The HW3 superheat is not negatively affecting the system since the ODU measurements are above zero. Found to be practiced in the industry, intentions are for at least 7°F to warrant consistent vapor into the compressor.

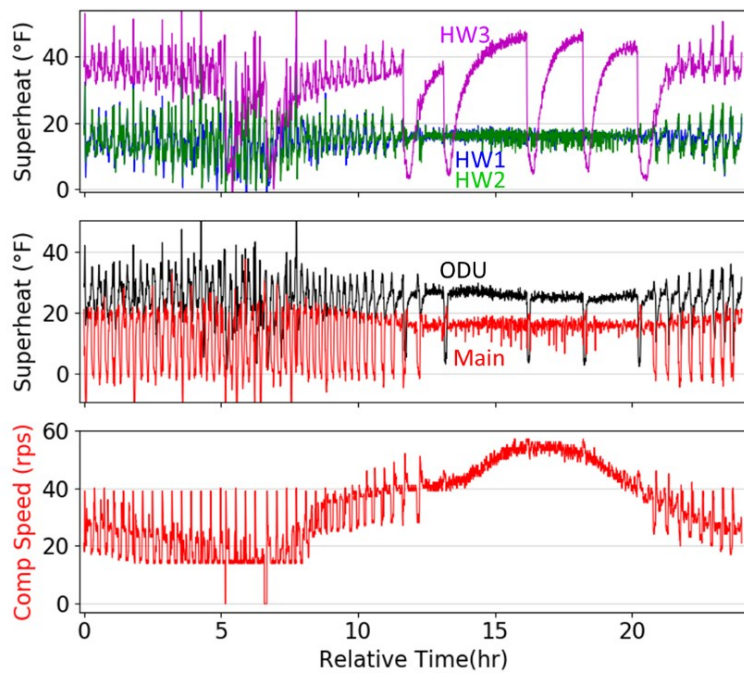


Figure 18. Compressor speed and superheats (Scn. A)

Figure 19 shows the temperature and pressure for each side of the ODU lines of suction and liquid. As an indicator of system operation, the individual pressures and temperature would migrate toward one another in search of equilibrium and spikes throughout are from various states of operation of the system. When the system calls for another component to ‘Cool Join’, the EEV is opened and creates a rapid pressure differential that is regulated by the compressor as it is prepared from the control algorithm to increase in speed due to incoming pressure changes.

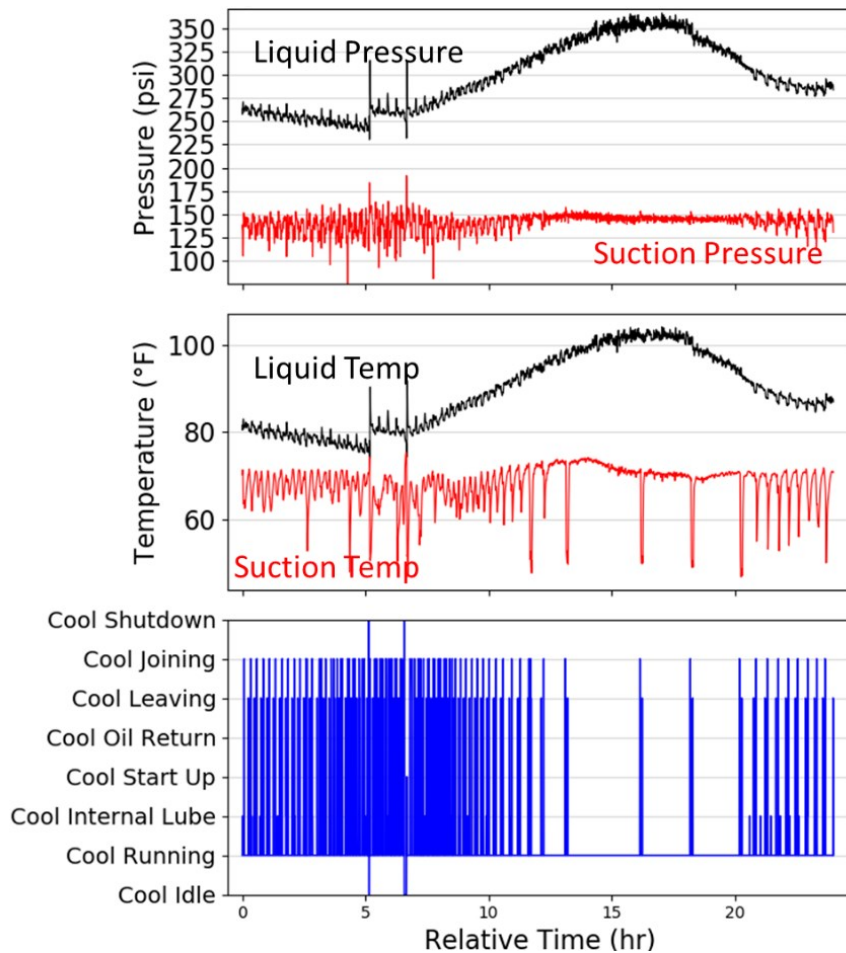


Figure 19. System state with line pressures and temperatures (Scn. A)

Scenario A'. Auxiliary measurements of vertical temperature stratification and grid temperature measurements on the wall in the living room with the ceiling fan off and on. The introduction to turning on the ceiling fan was an observational aspect under same operating conditions. Figure 20 shows living room data for two separate days that have the ceiling fan on and off. The control temp is kept below the set point enough to withstand being called while HW1 remains to be delivering the demanded capacity throughout.

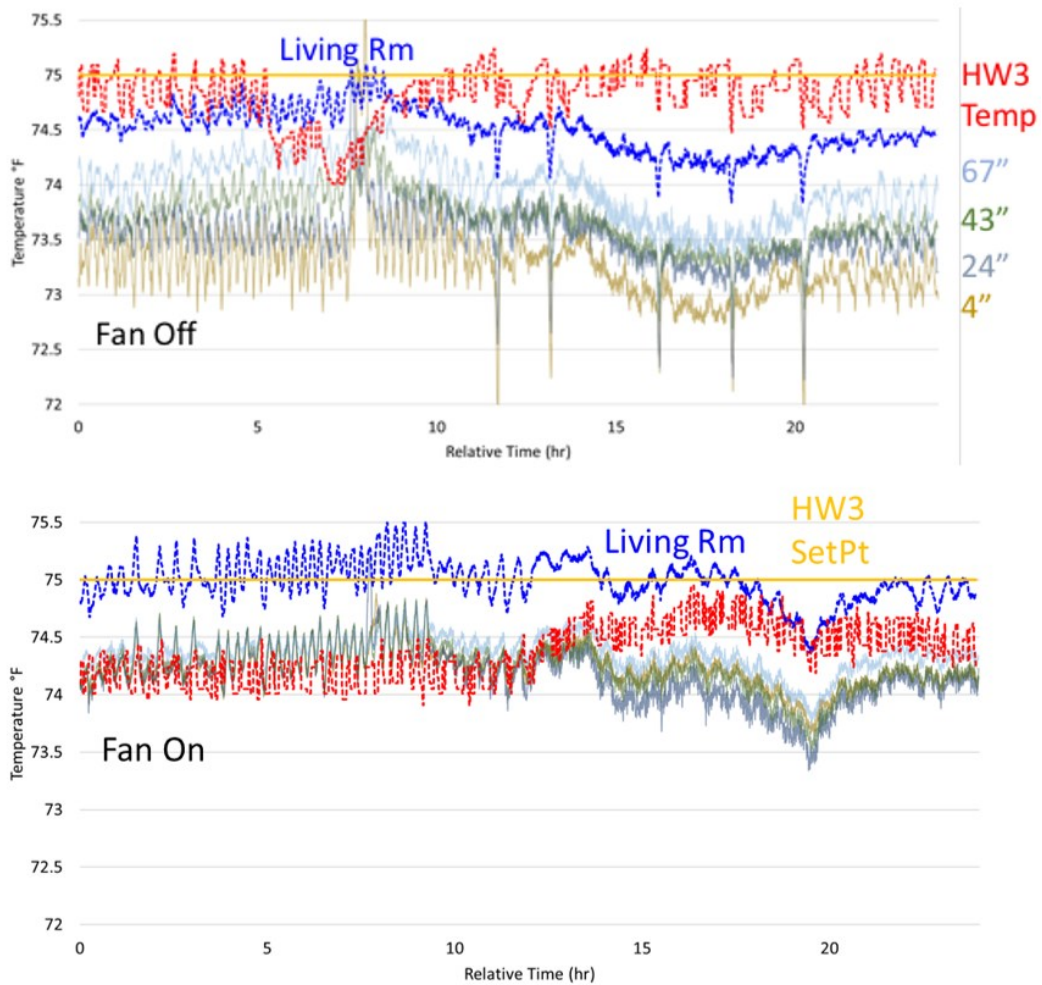


Figure 20. Vertical temperature stratification (Scn. A')

As the ductless zones HW1 and HW3 share an open floor plan, there is undoubtedly air mixture so the positioning of the vertical stratification apparatus can be affected by flowing air from the other zones even when the locations specific zone (living room) is not called for. This explains the living room average (blue) to be higher than the stratification measurements. Comparing between fan on and off modifiers of **scenario A** it can be observed that the ceiling fan operation certainly reduces the temperature difference between 4" (ankle) and 67" (head) to a span on average of 0.5°F during high demand times. In addition, the control temperature (red) has less noise and does not introduce any operation spikes as the temperature at the unit is maintained below the set point due to HW1(Kitchen) handling the demand throughout. While ceiling fan operation cannot by any means be recommended to the consumer there are only advantages to its operation as less searching for a target temperature is present while it is on.

In conjunction with the vertical stratification, Figure 21 is the alternate auxiliary measurement system of a temperature grid for potential controlling temperature sensor (thermostat). It shows similar temperature trends with respect to height changes when the ceiling fan is off. The height of the rows on the grid go 43", 55" and 67". These measurements are nearly 1°F warmer as these sensors are practically flush with the wall under the zones' highwall unit.

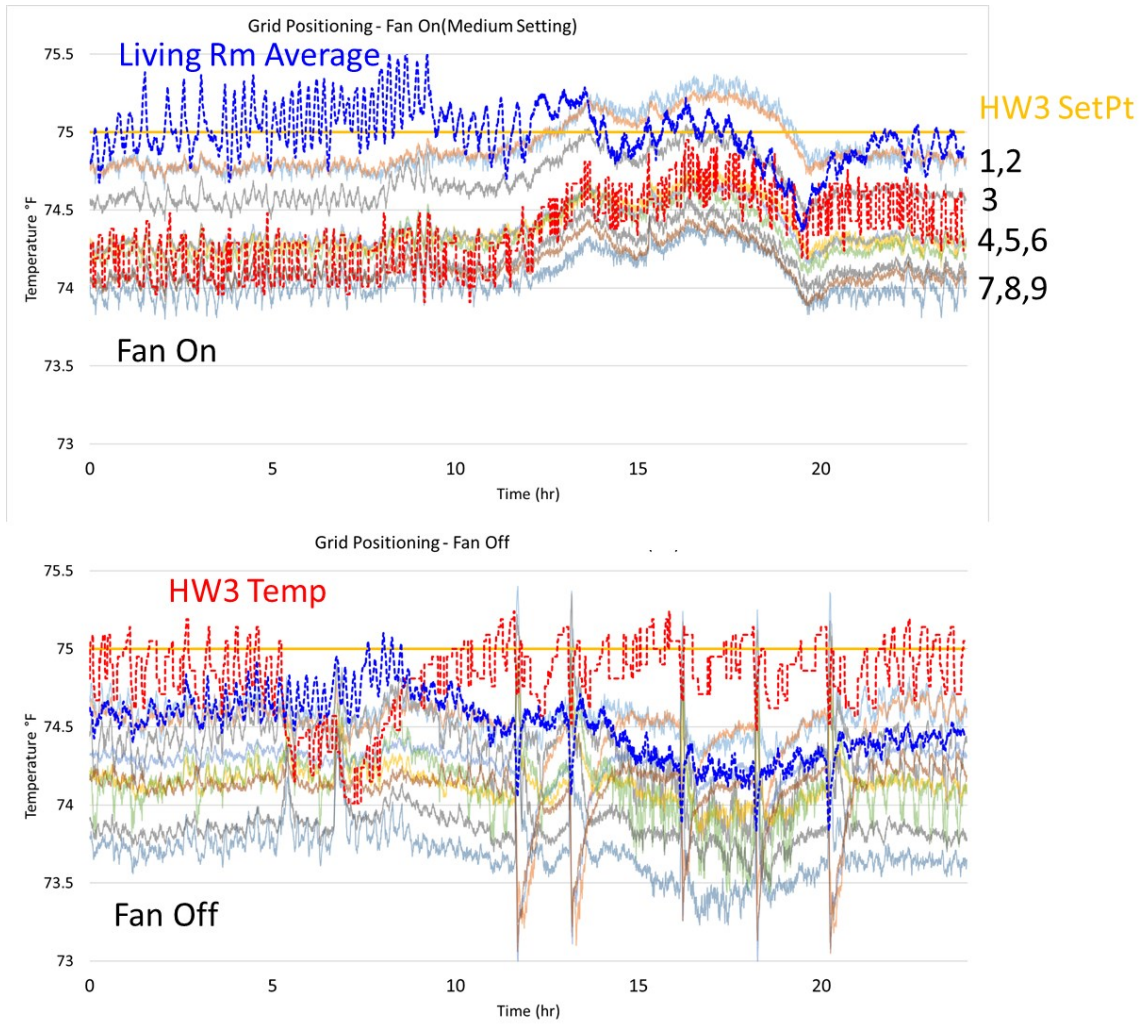


Figure 21. Temperature grid along living area wall (Scn. A')

Scenario B.

- One HW unit at 5°F set point difference.
- Target set points: Main = 75°F, HW1 = 75°F, HW2 = 75°F, HW3 = 70°F

Testing **scenario B** was put in place to monitor how the system would respond when one component had a lower set point of 5°F. In this case, HW3 (living room) was set to 70°F target while the other zones were kept at 75°F. Figure 22 shows the general system response of demand and the zone averaged temperature response throughout the day. Since HW1 and HW3 ultimately have a larger shared zone there lies influences from one unit to the other.

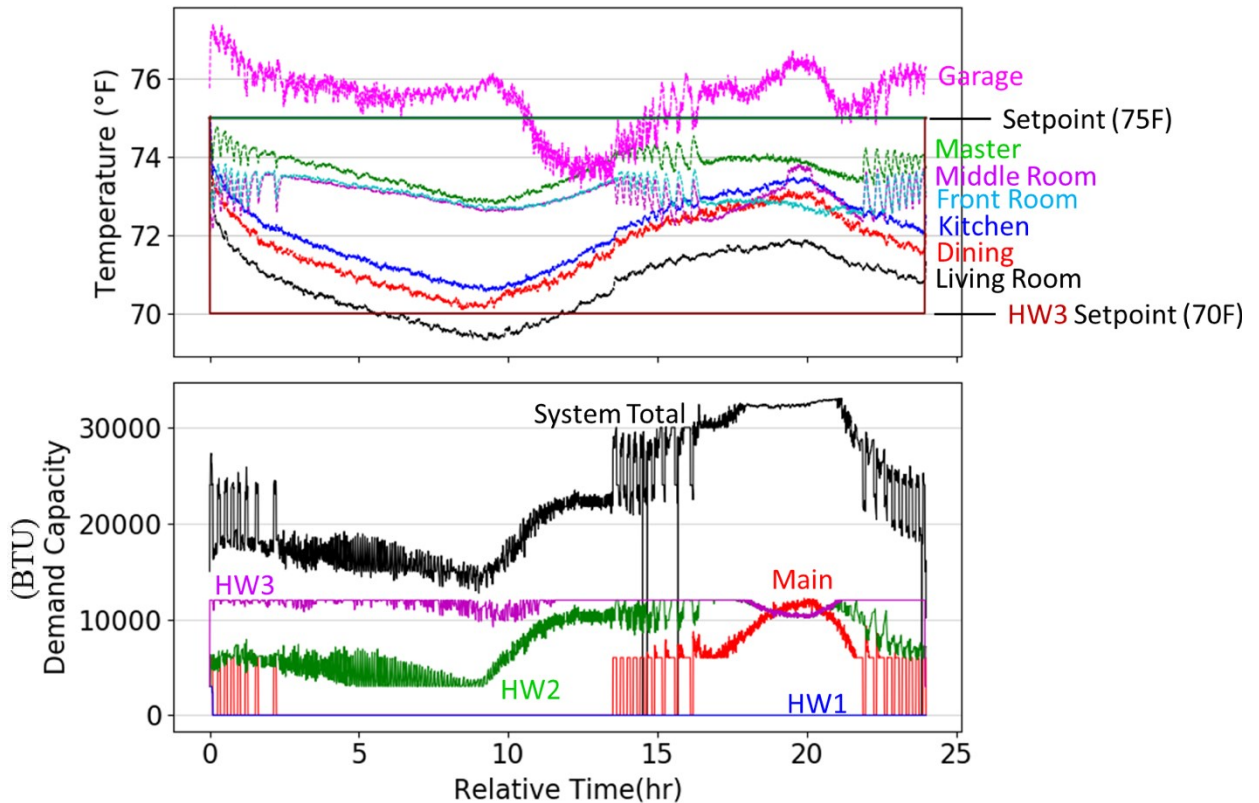


Figure 22. Demand capacity and zone temperatures (Scn. B)

HW3 is nearly at max capacity throughout this day of testing. From the zone average temperatures of Figure 22, the target of 70°F had potential to be reached overnight before the days hotter weather settled in. Pertaining to the ductless zones, HW1 was never called for during this test as HW3 was striving to reach its own target and inadvertently cooled the surrounding kitchen zone below its target. When outdoor temperature has risen and the AHU for the ducted zones has been called for the system is operating at max capacity and chooses to reallocate demand until targets are met in the ducted (main/bedrooms) zones while the HW3 (living room) remains at max capacity. This trend is what readjusted original testing plans for scenarios C and E. Analyzation would not have done much for this hybrid system rather than just a normal evaluation of a single mini-split system.

Scenario B superheat measurements illustrate a better understanding as indoor components remain off for longer periods of time shown in Figure 23. HW1 remains off during whole 24 hours of testing thus the superheat fluctuates with adjacent system refrigerant response since the refrigerant is filled but not flowing. The superheat at the Main's AHU is well above range due to inactivity and when activated immediately falls into range and remains during its operational duration. The compressor speed is not a smooth hill-like entrance to the higher demand portion of the day as the demand is being adjust and dispersed to the Main AHU unit until a constant conditioned airflow is required then the compressor speed increases to max constantly without modulation and cycling.

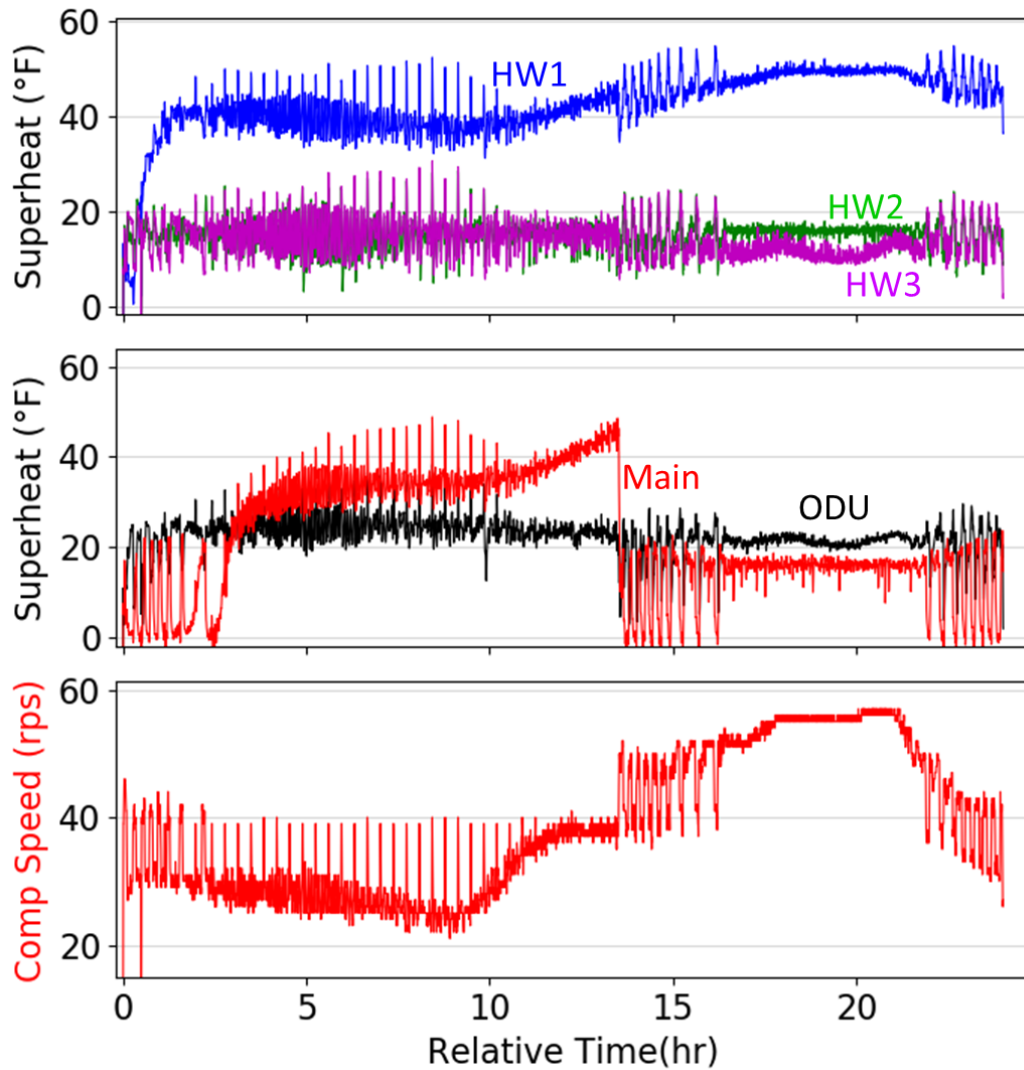


Figure 23. Compressor speed and superheats (Scn. B)

Scenario C.

- One HW unit at 10°F set point difference.
- Target set points: Main = 80°F, HW1 = 80°F, HW2 = 80°F, HW3 = 70°F

Scenario C was quickly overridden based on results of scenario B. This large of a set point difference kept HW3 on 100% while others indoor units remained inactive entirely and produced tangential results compared to scenario B.

Scenario D.

- All zones at normal different set points within 3°F
- Target set points: Main = 72°F, HW1 = 78°F, HW2 = 78°F, HW3 = 75°F

After seeing that a set point difference of 5°F from scenario B that would keep a neighboring zone below targets, attempting to find what set points would grant a good system response is where **scenario D** begins to find out where that threshold is. Figure 24 shows a two-day overview that was used for this testing scenario where the compressor remained on for the duration of the test with a quick system reset near end of the second day.

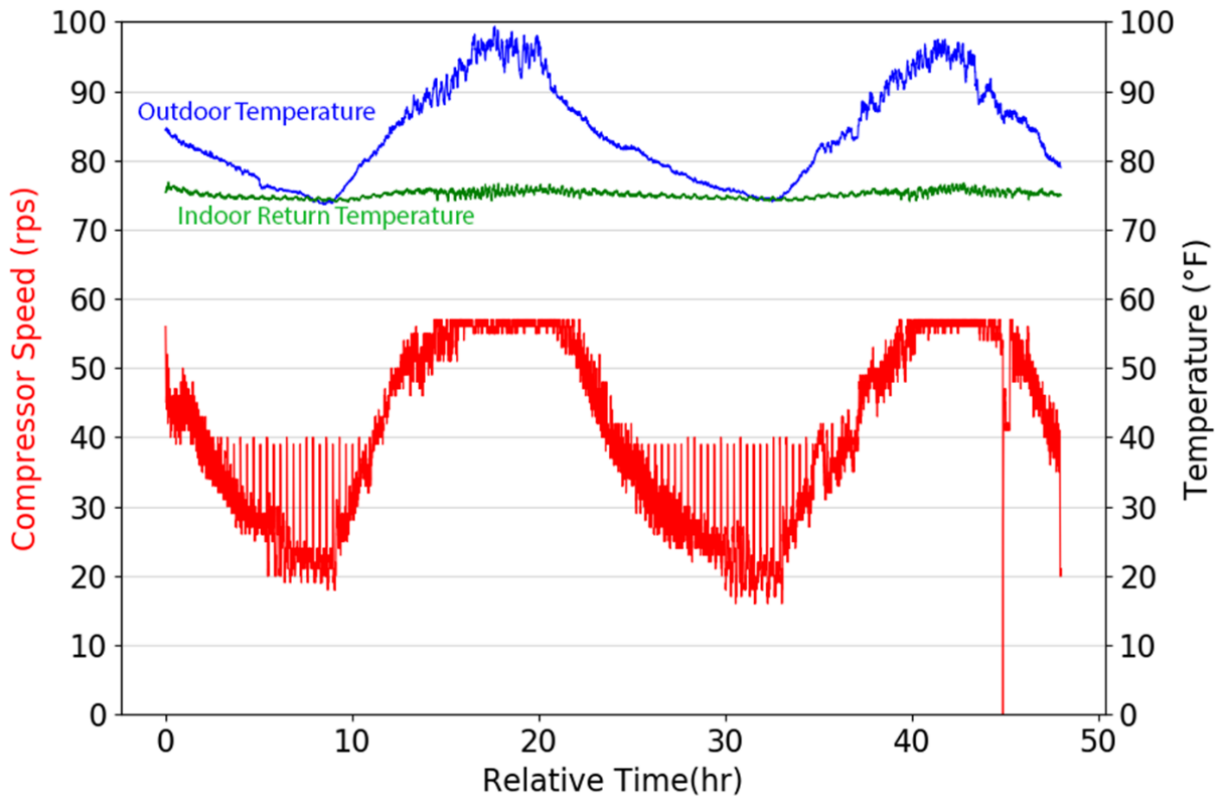


Figure 24. Two-day overall data (Scn. D)

Scenario D encountered issues among the highwall unit in the living room. In order to better understand the issue discovered, knowing how the system responds to demand is shown in Figure 25 over the course of two days. As the HW1 set point is higher than HW3, it was expected that HW3 would dominate control or at the very least turn on before HW1. In this case HW3 does not turn on at all while HW1 controls when the AHU for the ducted zones can no longer maintain temperature throughout the house near HW1.

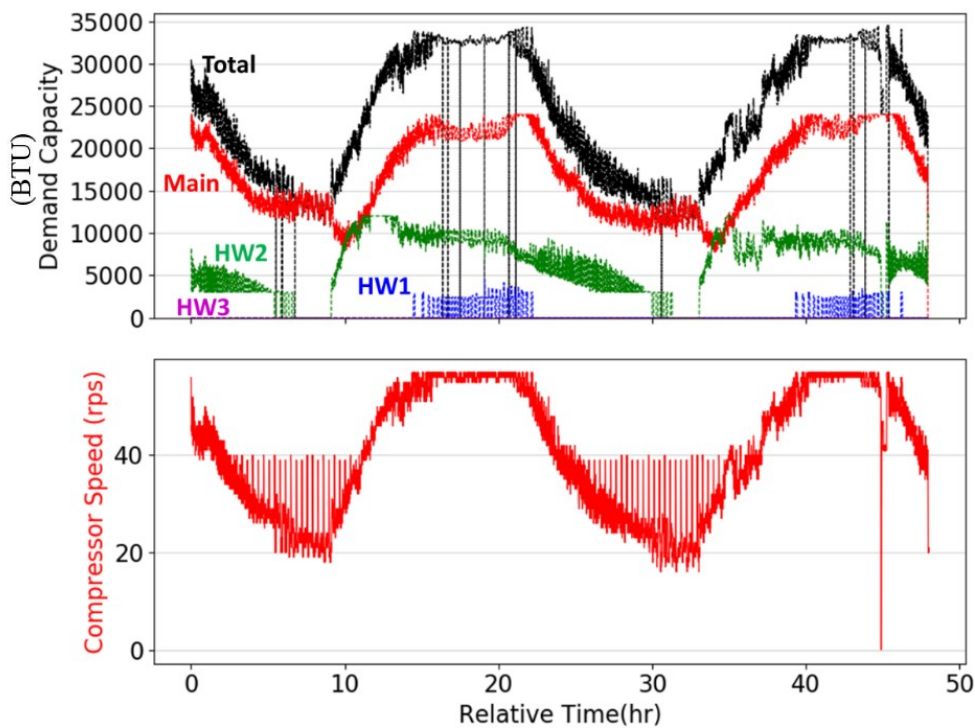


Figure 25. Compressor speed and demand capacity (Scn. D)

To discuss how issues were discovered, superheat measurements in Figure 26 are shown for this scenario. The superheat behavior of HW3 (purple) should have had similar trends to that of HW1 (blue) as increased superheat measurement when inactive. HW3 maintains superheat in the range of 5°F to 10°F while inactive. This leads to the ODU not

receiving refrigerant in its proper phase. It was found out that the indoor units' EEV was leaking refrigerant when the EEV was reporting a closed position. After reporting this a software fix was implemented that reinitialized its position to ensure it started counting steps of position accurately.

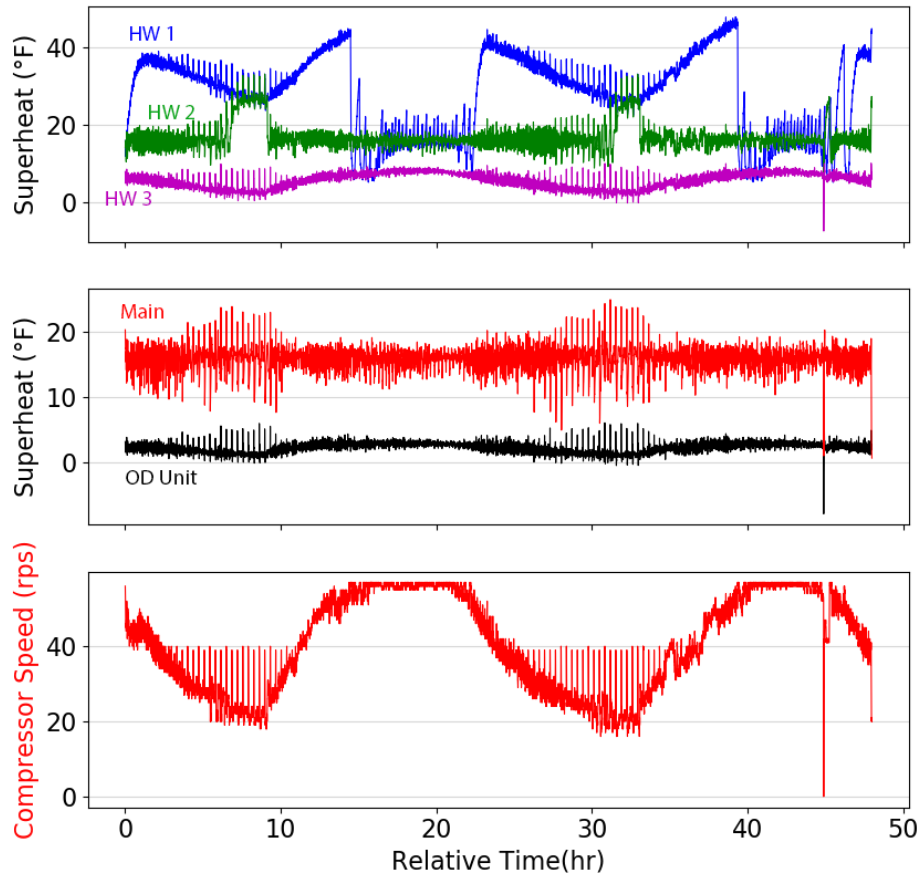


Figure 26. Compressor speed and superheats (Scn. D)

Scenario E.

- All zones at critical different set points of 5°F
- Target set points: Main = 70°F, HW1 = 80°F, HW2 = 80°F, HW3 = 75°F

Scenario E, similar to C, was overridden for the same reasons of tangential results to scenario B.

Scenario F.

- All zones at same set point with a change in one indoor unit midday
- Target set points: Main = 75°F, HW1 = 75°F (down to 70°F), HW2 = 75°F, HW3 = 75°F

This testing scenario was treated as predictable response by end users arriving home near end day and adjusting zone set point. In **scenario F**, the set point change midday can be seen in Figure 27 nearing 3 PM with a compressor trend overnight that has yet to be seen. This overnight ambient temperature was one of the cooler nights during the summer which dropped below desired indoor temperatures at times. This caused the system to cycle on and off rather than stay at minimum speed as has been seen in previous scenario results.

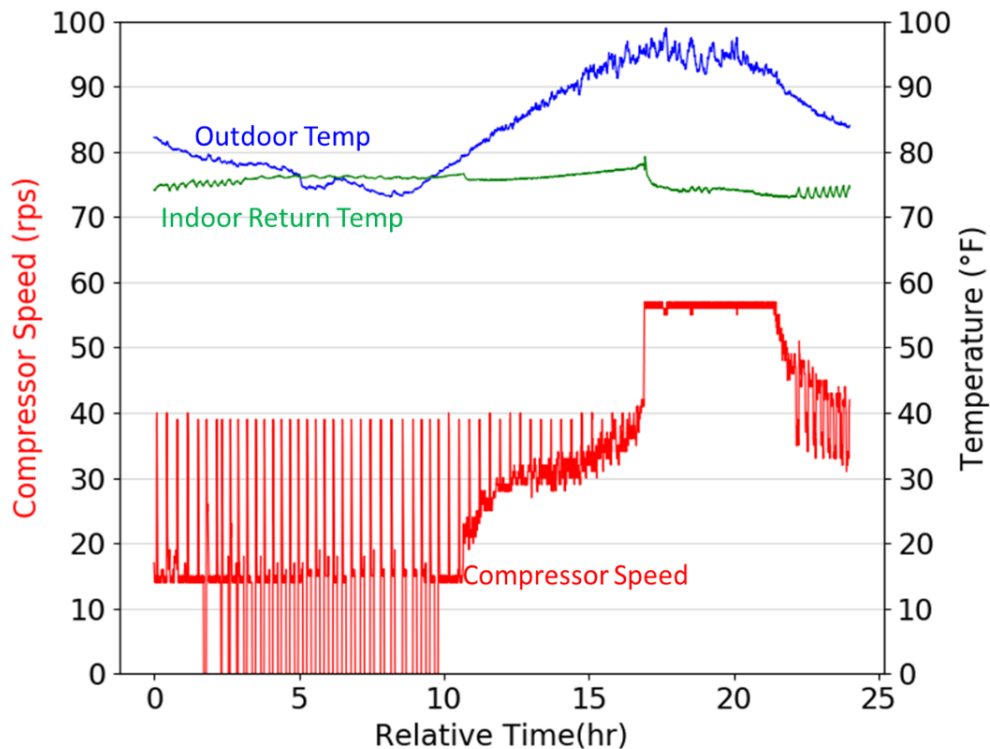


Figure 27. Overall daily data (Scn. F)

The top range of the cycling trend is just shy of 40 rps, which is the designated start up speed and internal lube speed. This compressor is programmed to begin at 40 rps when initialized and internal lube which oils the compressors internal components to keep it running safely and smoothly. The average indoor temperature began to drastically decrease as the set point was adjusted to 70°F of HW1. Demand capacity was normally increasing with outdoor ambient temperature then when the conditional set point was adjusted the capacities had to be appropriately divided with the allotted maximum capacity near 34,000 BTU, shown in Figure 28 with zone averaged temperatures and control temperatures.

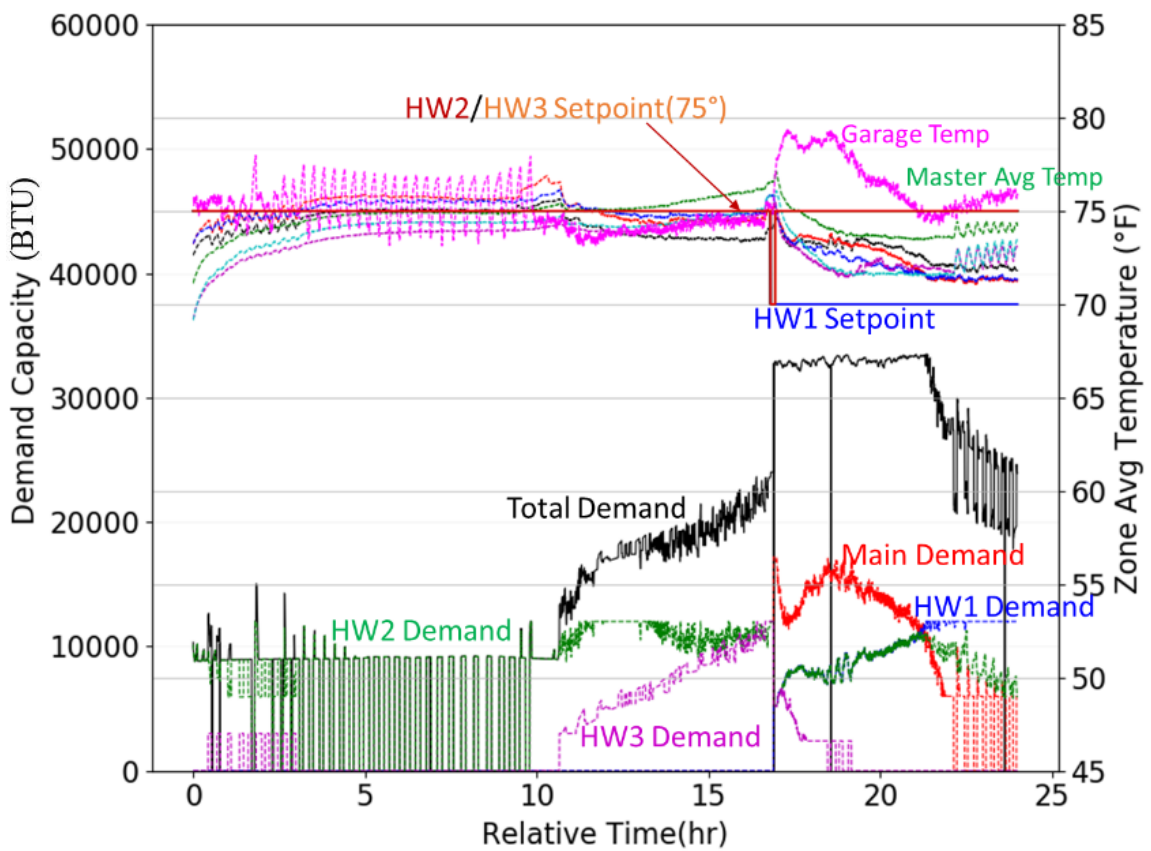


Figure 28. Demand capacity and zone temperatures (Scn. F)

Figure 29 shows the fineness of pressure and line temperature up until the midday set point change that altered the system operation. After the set point change, the only system state changes were when HW units and the AHU controlling set points were met to adjust the system state to ‘Cool Leaving’ when an indoor unit turned off. At near full capacity the system regulates pressure and temperature better than when specific system components are active.

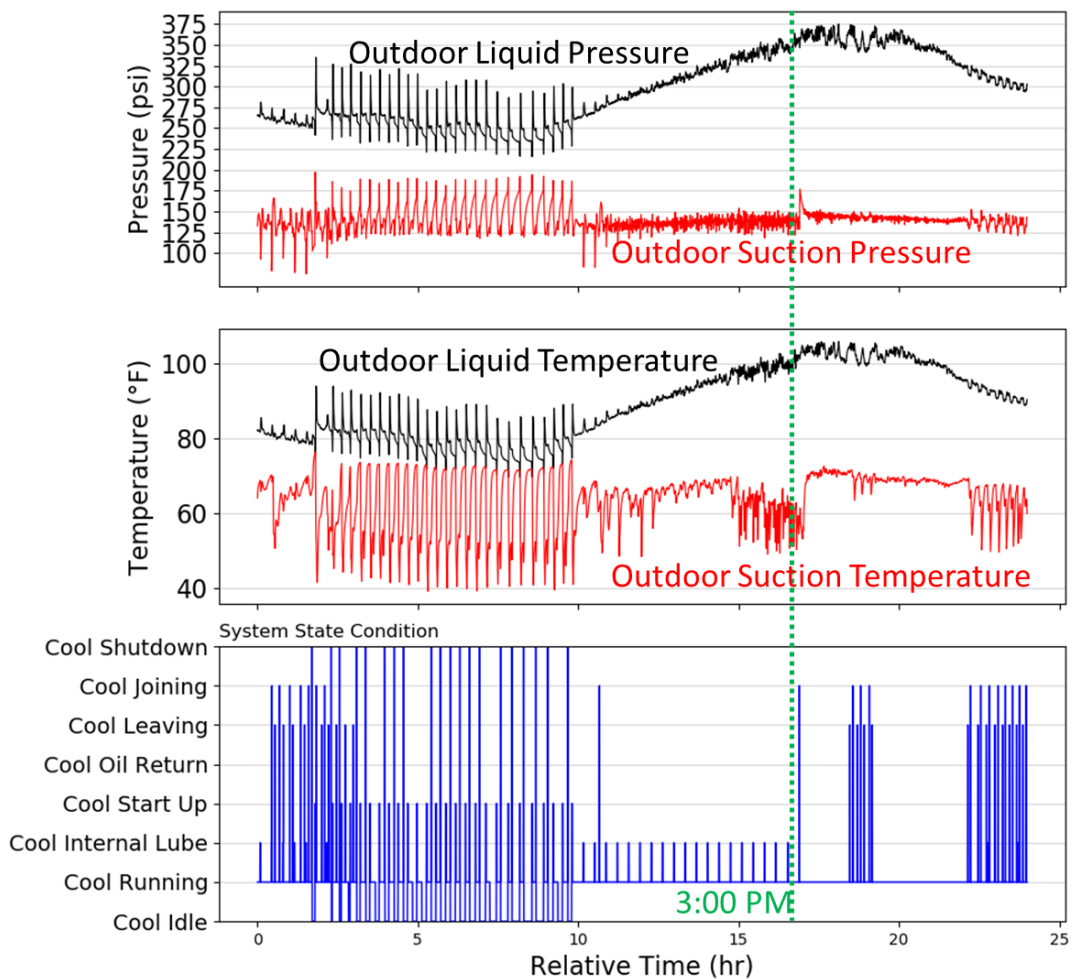


Figure 29. System state with line pressures and temperatures (Scn. F)

Scenario G.

- All zones at normal different set points within 2°F
- Target set points: Main = 76°F, HW1 = 74°F, HW2 = 74°F, HW3 = 72°F

Scenario G was taken over two days as a direct derivation to scenario D with a smaller difference in set points between zones. Overview data was similar, so investigation continued on spatial response throughout zones and system operational response. Figure 30 is of the ductless zone temperatures with HW unit control temperatures.

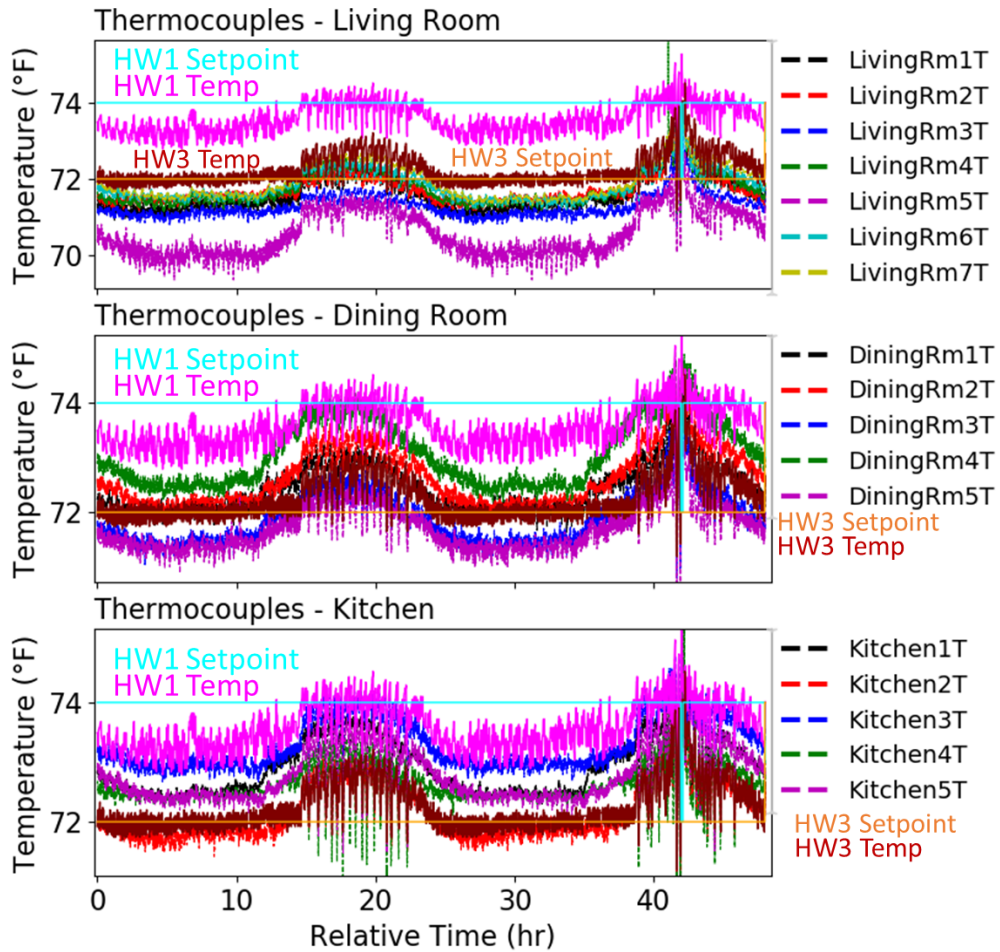


Figure 30. Ductless (HW) temperatures (Scn. G)

With HW3 having the lowest set point of 72°F (HW1=74°F, HW2=74°F, Main=76°F), the control temperature for HW1 is show to be constantly under target with exceptions during hottest part of the day where there are peaks of control temperature above 74°F. HW3 control temperature trend is concise and keeps every thermocouple below 74°F. This comes of course with HW3 being on 100% of the testing duration as shown in Figure 31 with spikes of operation from HW1 and Main AHU zones but only during highest demand portion of the day.

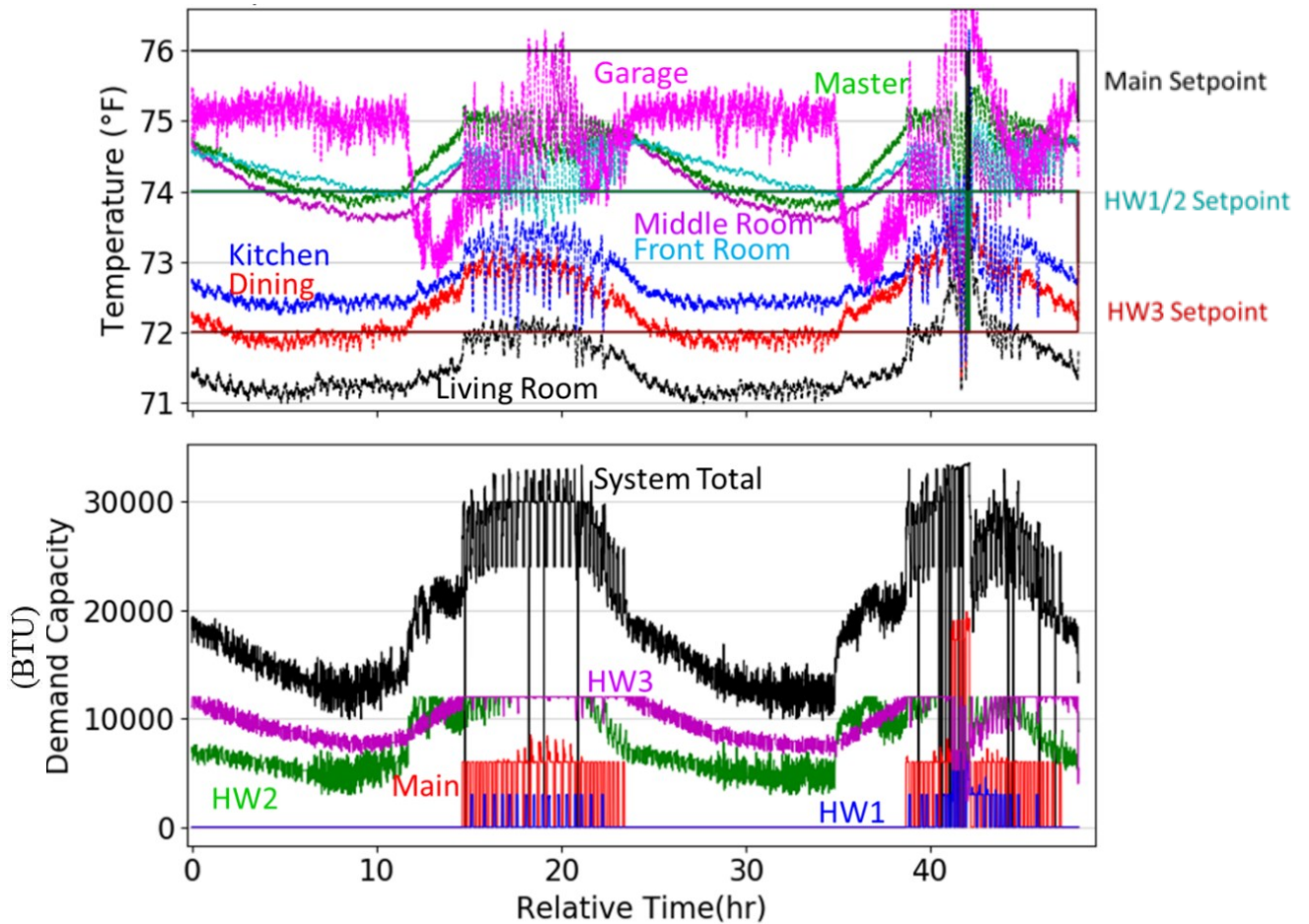


Figure 31. Demand capacity and zone temperatures (Scn. G)

Compared to scenario D, that was within 3°F of each set point held off the alternate HW unit out of operation during the entire test. Control is working well when demand is increasing and requiring zone allocation for different set points. It is seen the HW3 cannot handle entire house capacity at its highest thus requires aid to maintain specifications. Figure 32 is of compressor speed and superheat measurements after the HW3 issue of the EEV leaking refrigerant had been fixed and reporting proper superheat ranges, particularly that the ODU is receiving only vapor into the compressor.

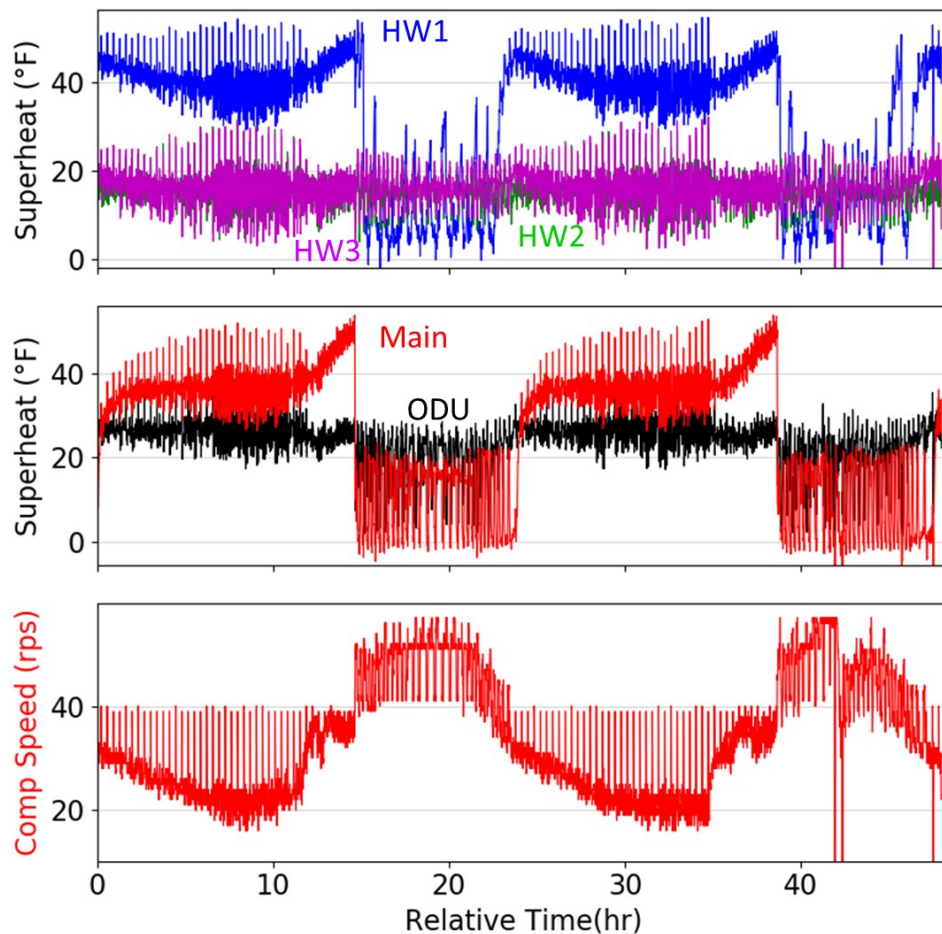


Figure 32. Compressor speed and superheats (Scn. G)

Scenario H.

- All zones at normal different set points within 1°F
- Target set points: Main = 75°F, HW1 = 73°F, HW2 = 73°F, HW3 = 74°F

Scenario H, also a two-day period, is a closer range of separate set points than that of scenario G. Lowering the threshold of set point differences to 1°F is where changes in indoor components should be more frequent in **scenario H**. From a temperature controller perspective there was a larger span of time where HW3 was above set point and calling for airflow as shown in Figure 33. Across the testing time, HW1 mostly maintained the ductless zone air temperature below the 74°F threshold for HW3 to turn on.

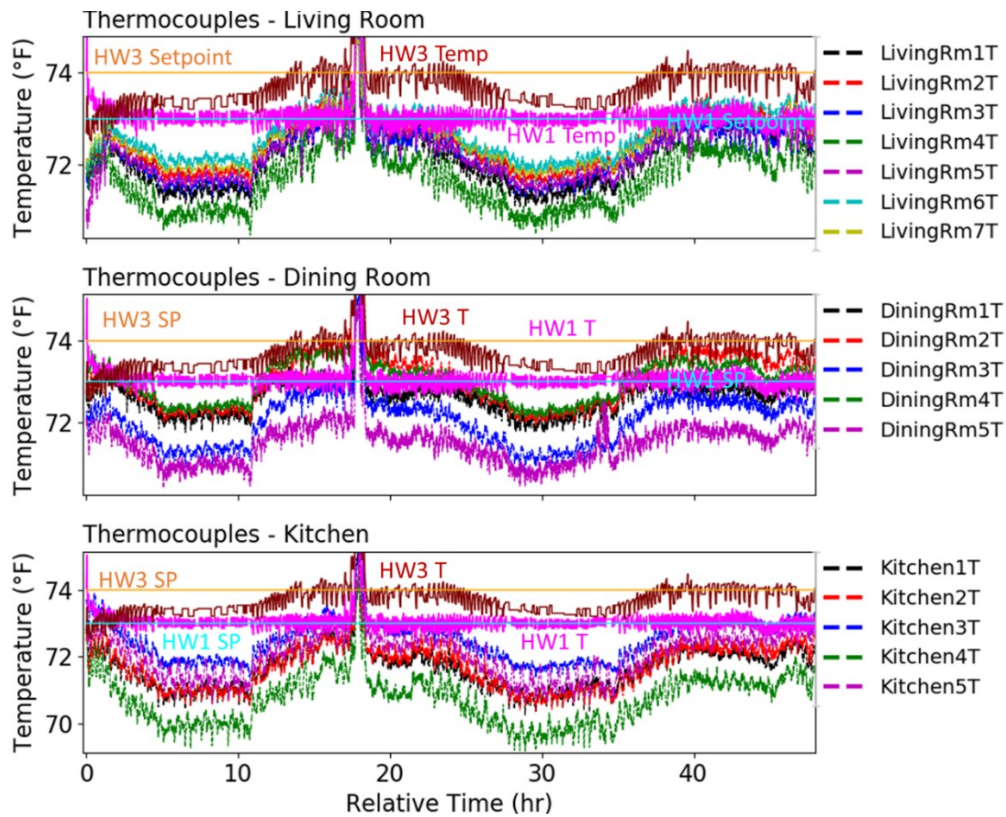


Figure 33. Ductless (HW) temperatures (Scn. H)

Figure 34 shows where the response of the higher set points zones, HW3 and Main, begins earlier and ends later than previous testing scenario G with more control instead of simply turning on then off again to maintain some minimal airflow. For zone averaged temperatures, the air temperature in the front and middle bedroom closer relates to the master zone temperature from previous duct dampening methods.

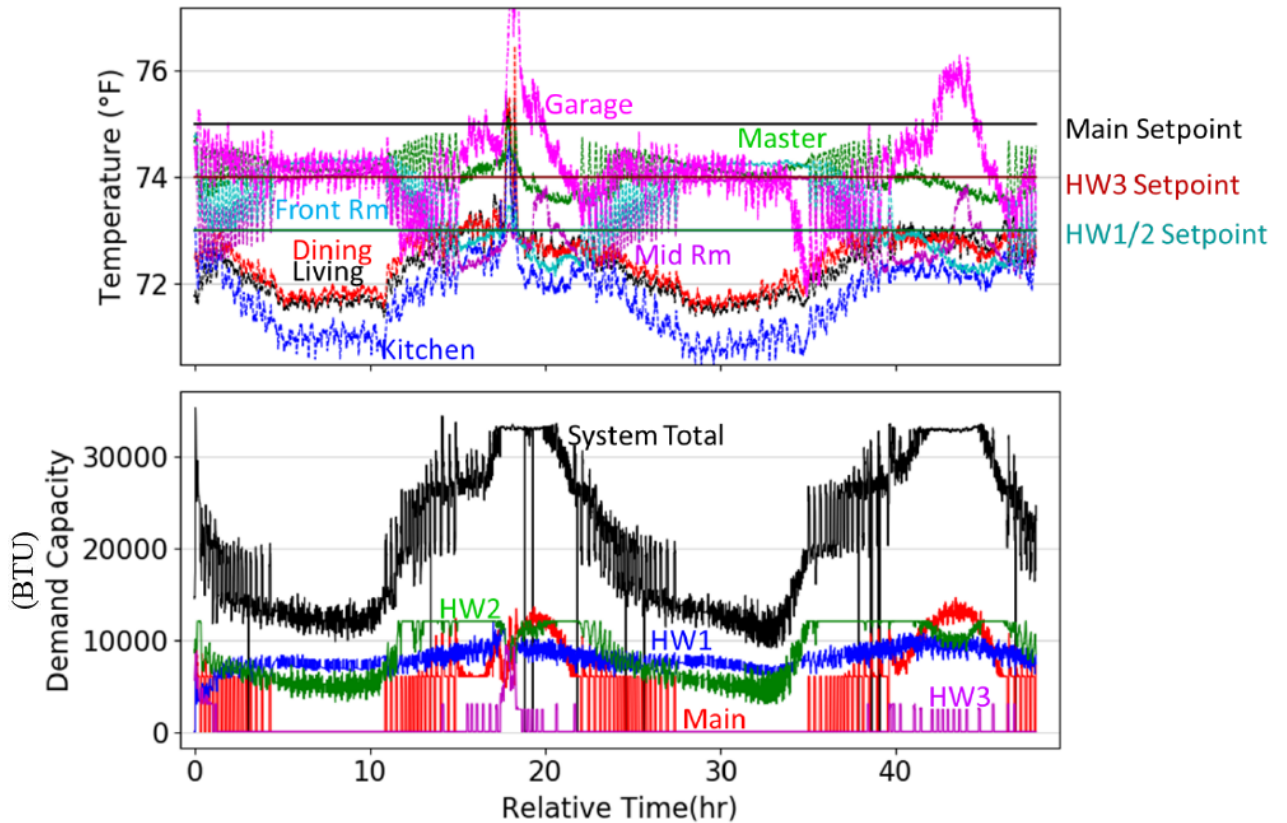


Figure 34. Demand capacity and zone temperatures (Scn. H)

HW1 and HW2 superheat were maintained at around 15°F with alternate indoor units and AHU activating during high demand and an acceptable range into the ODU compressor taken from Figure 35. Throughout the derived scenarios of D, G, and H

superheat control was within range when EEV positioning was fully operational and not leaking refrigerant.

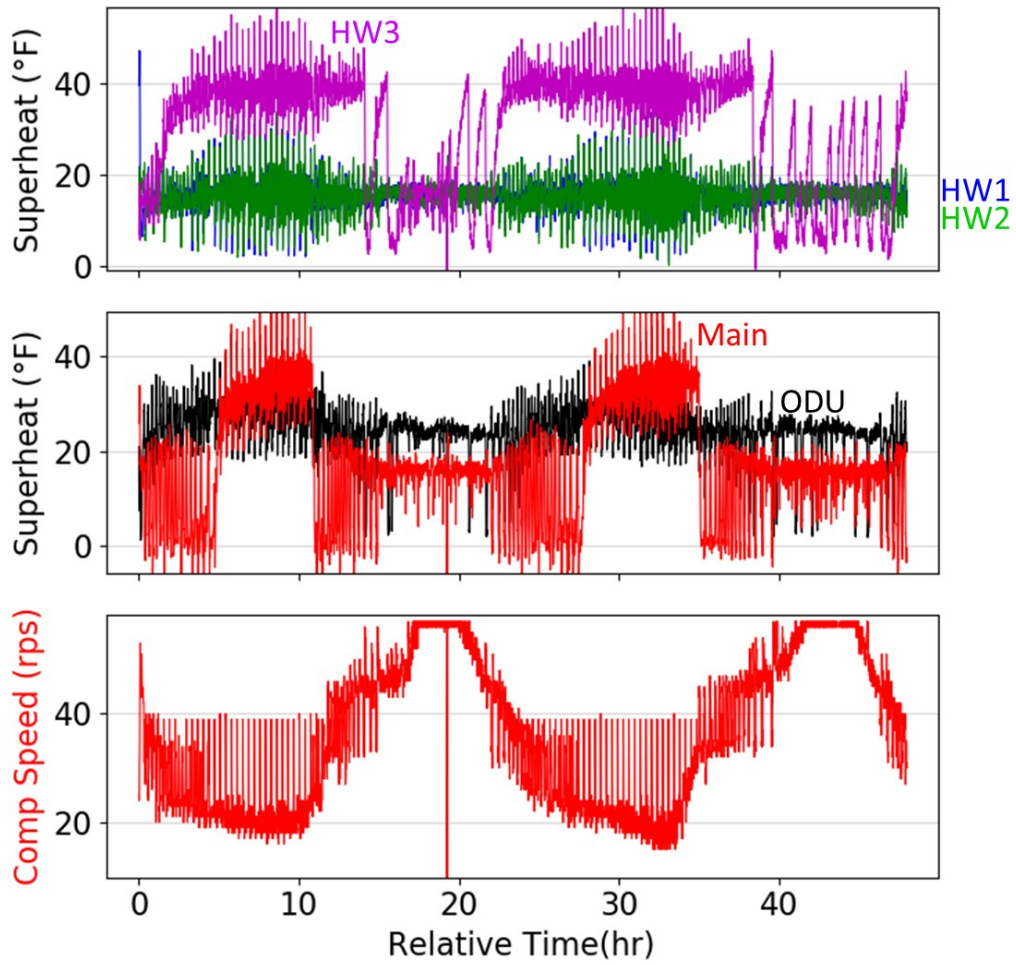


Figure 35. Compressor speed and superheats (Scn. H)

Peripheral Data.

This section includes slides that are not particular to the list of scenarios, however, were utilized throughout the process for a variety of reasons. Figure 36 is an example of poor daily data where the compressor ceased operation around 2 AM and fixed and reinstated around 1 PM. Occurrences similar to these were evaluated with Trane personnel to find out where the system failure took place and if it is repeatable to fix it in either hardware or software.

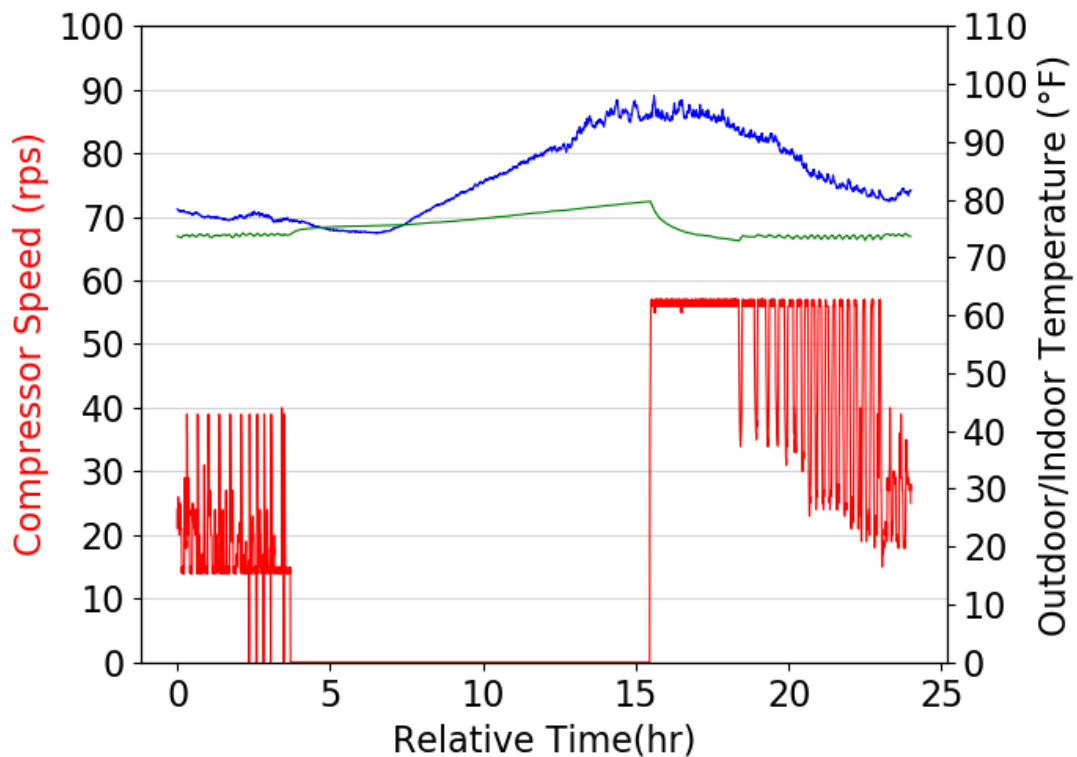


Figure 36. Daily overview of system failure and data

Figure 37 is an example of a layout used to evaluate each of relevant variables at times of failure or stoppage. This shows the zooming advantage to using python scripting (with relevant coding libraries) over excel. The figure time span is for only 1 hour and

specifically at this point to check how EEV positioning and superheat respond to demand and airflow changes.

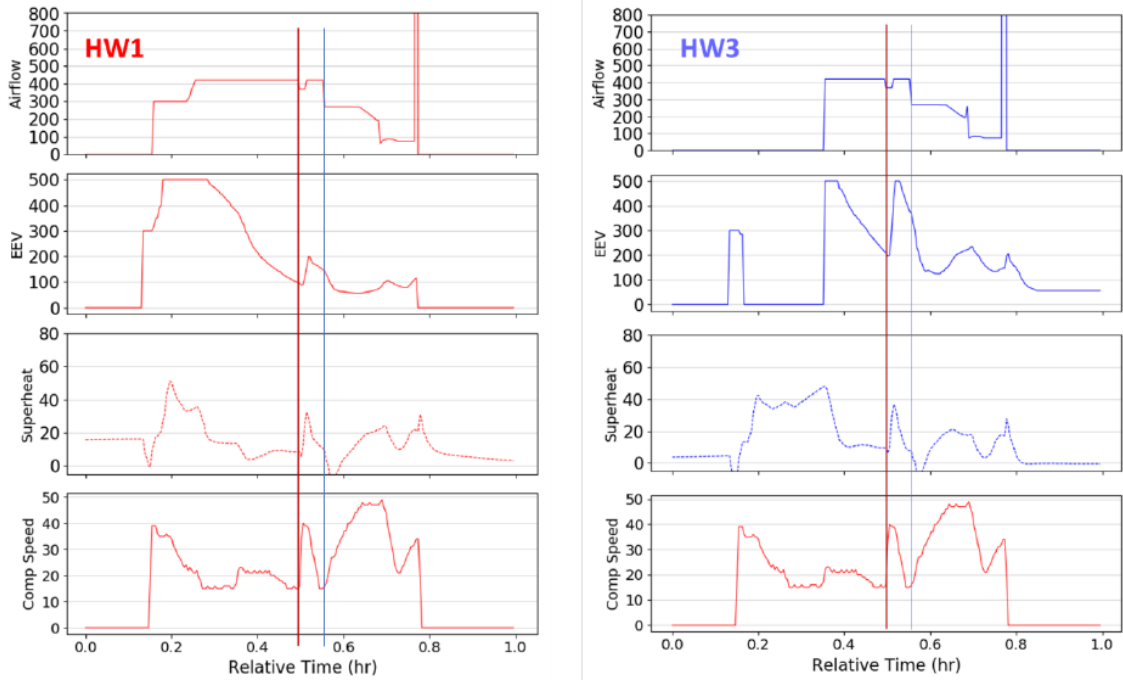


Figure 37. Troubleshooting sample

Chapter 5

Conclusions and Recommendations

Developing a testing method for a system that has yet to be defined in the market could only be generalized from practices that have been done per individual components. This hybrid ducted-ductless HVAC introduced challenges as having monitor multiple evaporator units simultaneously and the overall synergy with the conducted tests. Continuous feedback of system operations further aided in defining the levels of dynamic intricacy for testing scenarios. Following guidelines from ASHRAE and NREL set a foundation for testing protocols tailored to this project with help of TRANE engineers.

Throughout testing scenarios data collection in erroneous system statuses began to prove more valuable as components began to pose issues that would render zones inactive for an extended period of time. As this system is in development, there are various stages where controlling software takes precedence in order the system remains safely operational.

Single set points for each component maintained good control to maintain desired comfort in the house on a day to day basis. Specific caveats relate to accuracy and consistency of a select few controlling sensors that dictated how well certain testing scenarios were concluded.

Attempts to individualize zones for the ductless components had limitations since two highwall units shared an open floor plan thus mixing air from one units' zone to its neighbor. Testing scenarios were eventually realized that the difference in zone set points

cannot exceed a certain value otherwise one high wall unit would dominate all of the ductless zones not allowing demand to be called for testing purposes. While this does prove a particular unit can uphold comfortability it does not explicit prove the system can control various parameters per zone.

With this developmental project, the path at times was obscured as data from specific testing scenarios resulted in an immediate action in regard to software changes that was ever adapting throughout this time period. As time went forth with this season, changes were made in both hardware and software. New controlling algorithms were not able to be fully implemented and finely tuned by the creator. This forms an opening path of actions for the following season as the supplementary hardware changes will support the progression of testing and analysis. From the tools acquired and knowledge gained through successes and failures, future work should expect refined results with understanding how the 2018 summer season testing scenarios responded. The discussions held throughout the season aided in learning to promote relevant data for expert review. While in the academic environment there has always been solutions to given problems, however in this project and related research there is no specific solution and often seems trying to understand the correct path to follow for success.

References

- [1] J.-L. Lin and T.-J. Yeh, "Identification and control of multi-evaporator air-conditioning systems," *International Journal of Refrigeration*, vol. 30, pp. 1374-2385, 2007.
- [2] A. Sencan, R. Selbas, O. Kizilkan and S. A. Kalogirou, "Thermodynamic analysis of subcooling and superheating effects of alternative refrigerants for vapour compression refrigeration cycles," *International Journal of Energy Research*, vol. 30, pp. 323-347, 2006.
- [3] Q. Tu, L. Zhang, W. Cai, X. Guo, X. Yaun, C. Deng and J. Zhang, "Control strategy of compressor and sub-cooler in variable refrigerant flow air conditioning system for high EER and comfortable indoor environment," *Applied Thermal Engineering*, vol. 141, pp. 215-225, 2018.
- [4] S. Atas, M. Aktas, I. Ceylan and H. Dogan, "Development and Analysis of a Multi-evaporator Cooling System with Electronic Expansion Valves," *Arabian Journal for Science & Engineering*, vol. 42, pp. 4513-4521, 2017.
- [5] R. Shah, A. G. Alleyne, and C. W. Bullard, "Dynamic Modeling and Control of Multi-Evaporator Air-Conditioning Systems," *ASHRAE Transactions*, vol. 110, p. 109, 2004.
- [6] Q. Tu, D. Zou, C. Deng, J. Zhang, L. Hou, M. Yang, G. Nong and Y. Feng, "Investigation on output capacity control strategy of variable refrigerant flow air conditioning system with multi-compressor," *Applied Thermal Engineering*, vol. 99, pp. 280-290, 2016.
- [7] J. Xia, E. Winandy, B. Georges and J. Lebrun, "Testing Methodology for VRF Systems," in *International Refrigeration and Air Conditioning Conference*, 2002.
- [8] J. Choi and Y. Kim, "Capacity modulation of an inverter-driven multi-air conditioner using electronic expansion valves," *Energy*, vol. 28, pp. 141-155, 2003.
- [9] A. Alahmer and S. Alsaqoor, "Simulation and optimization of multi-split refrigerant flow systems," *Ain Shams Engineering Journal*, vol. 9, pp. 1705-1715, 2018.

- [10] A. Amarnath and M. Blatt, "Variable Refrigerant Flow: Where, Why, and How," no. 25, p. 54, 2008.
- [11] R. Saab, H. A. Quabeh and M. I. Hassan Ali, "Variable refrigerant flow cooling assessment in humid environment using different refrigerants," *Journal of Environmental Management*, vol. 224, pp. 243-251, 2018.
- [12] R. Saab and M. I. Hassan Ali, "Variable refrigerant flow cooling systems performance at different operation pressures and types of refrigerants," *Energy Procedia*, vol. 119, pp. 426-432, 2017.
- [13] J. Meng, M. Liu, W. Zhang, R. Cao, Y. Li, H. Zhang, X. Gu, Y. Du and Y. Geng, "Experimental investigation on cooling performance of multi-split variable refrigerant flow system with microchannel condenser under part load conditions," *Applied Thermal Engineering*, vol. 81, pp. 232-241, 2015.
- [14] H. Cheung and J. E. Braun, "Performance comparisons for variable-speed ductless and single speed ducted residential heat pumps," *International Journal of Refrigeration*, vol. 47, pp. 15-25, 2014.
- [15] D. Zhang, X. Zhang and J. Liu, "Experimental study of performance of digital variable multiple air conditioning system under part load conditions," *Energy & Buildings*, vol. 43, pp. 1175-1178, 2011.
- [16] B. Min, S. Na, T. Lee, S. Jang, H. Bae, C. Moon and G. Choi, "Performance analysis of multi-split variable refrigerant flow (VRF) system with vapor-injection in cold season," *International Journal of Refrigeration*, vol. 99, pp. 419-428, 2019.
- [17] P. Yan, X. Xiangguo, X. Liang and D. Shiming, "A modeling study on the effects of refrigerant pipeline length on the operational performance of a dual-evaporator air conditioning system," *Applied Thermal Engineering*, vol. 39, pp. 15-25, 2012.
- [18] H. Yan and S. Deng, "Simulation Study on a Three-evaporator Air Conditioning System for Improved Humidity Control," *Energy Procedia*, vol. 105, pp. 2139-2144, 2017.
- [19] D. Park, G. Yun and K. Kim, "Experimental evaluation and simulation of a variable refrigerant- flow (VRF) air-conditioning system with outdoor air processing unit," *Energy and Buildings*, vol. 146, pp. 122-140, 2017.
- [20] S.-C. Hu and R.-H. Yang, "Development and testing of a multi-type air conditioner without using AC inverters," *Energy Conversion and Management*, vol. 46, pp. 373-383, 2005.

- [21] J.-L. Lin and T.-J. Yeh, "Control of multi-evaporator air-conditioning systems for flow distribution," *Energy Conversion and Management*, vol. 50, pp. 1529-1541, 2009.
- [22] W.-J. Zhang and C.-L. Zhang, "Transient modeling of an air conditioner with a rapid cycling compressor and multi-indoor units," *Energy Conversion and Management*, vol. 52, pp. 1-7, 2011.
- [23] Q. Tu, K. Dong, D. Zou and Y. Lin, "Experimental study on multi-split air conditioner with digital scroll compressor," *Applied Thermal Engineering*, vol. 31, no. 14-15, pp. 2449-2457, 2011.
- [24] H. Yan, S. Deng and M.-Y. Chan, "Operating characteristics of a three-evaporator air conditioning (TEAC) system," *Applied Thermal Engineering*, vol. 103, pp. 883-891, 2016.
- [25] ASHRAE, "55 - Thermal Environmental Conditions for Human Occupancy," ASHRAE, Atlanta, 2013.
- [26] ASHRAE, "113 - Method of Testing for Room Air Diffusion," ASHRAE, Atlanta, 2013.
- [27] ASHRAE, "70 - Method of Testing the Performance of Air Outlets and Air Inlets," ASHRAE, Atlanta, 2011.
- [28] D. Christensen, X. Fang, J. Tomerlin, J. Winkler and E. Hancock, "Field Monitoring Protocol: Mini-Split Heat Pumps," National Renewable Energy Lab, Colorado, 2011.
- [29] "National Instruments," 22 August 2017. [Online]. Available: <http://www.ni.com/tutorial/7114/en/>. [Accessed 2017].

Appendix A. Research Site



Figure A1. Research site signage



Figure A2. Research site with both residential houses



Figure A3. Front of VRF ducted-ductless HVAC system house

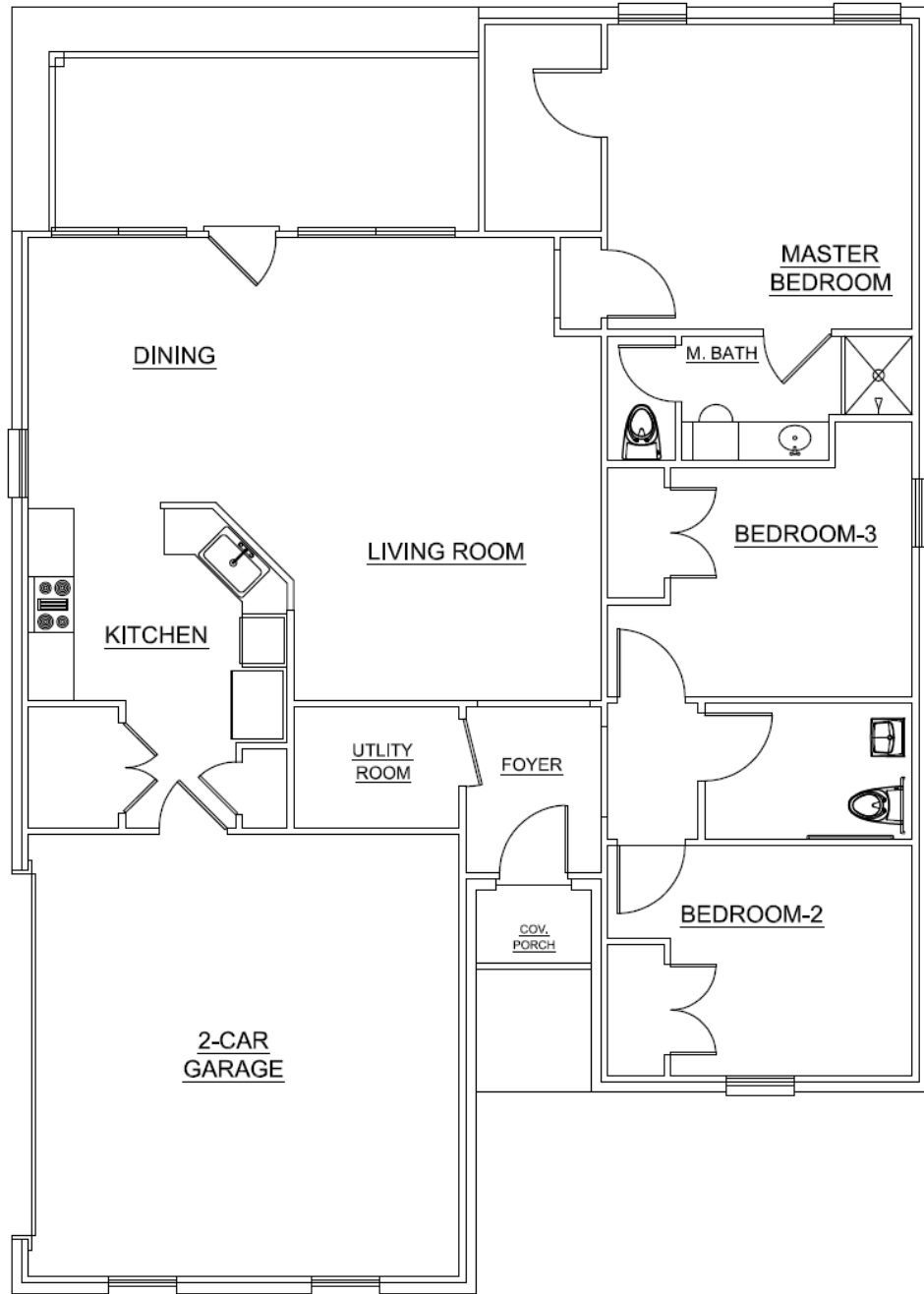


Figure A4. Technical floor plan of research house

Appendix B. Indoor images



Figure B1. Thermocouple hanging through acrylic tubing

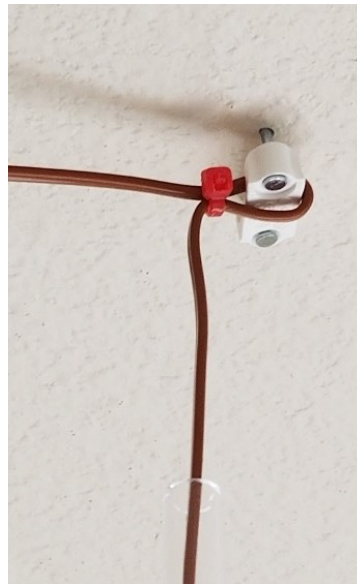


Figure B2. Thermocouple positioning from ceiling

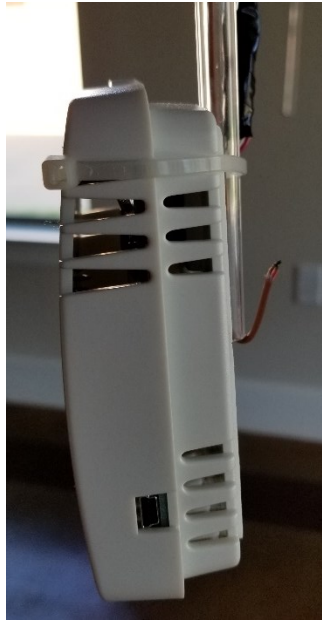


Figure B3. Thermocouple and relative humidity sensor



Figure B4. Master bedroom



Figure B5. Middle bedroom



Figure B6. Front bedroom



Figure B7. Dining room with repositionable thermocouple pole



Figure B8. HW3 in living room with temperature grid on wall



Figure B9. Airflow validation setup



Figure B10. Airflow measurement pressure hardware

Appendix C. National Instruments Hardware and Software



Figure C1. Used cRIO modules in NI-9074 chassis

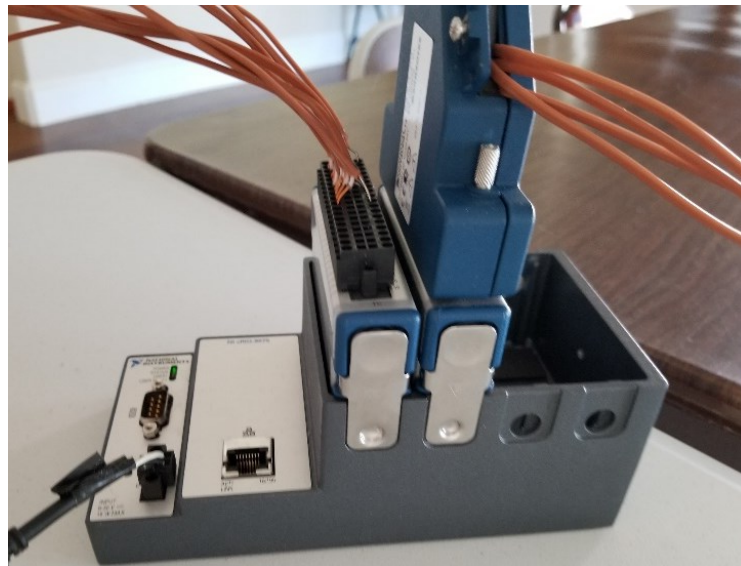


Figure C2. NI-9705 chassis with auxiliary measurement thermocouples

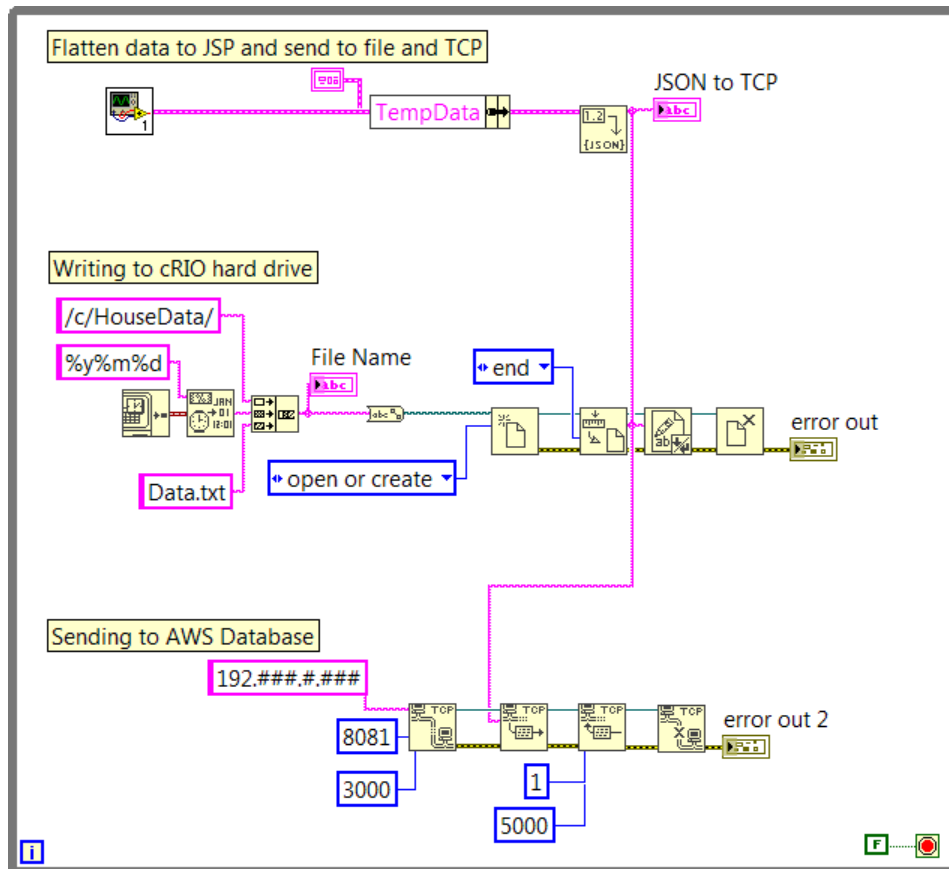


Figure C3. Data processing and forwarding VI

Appendix D. Complete Scenario Results

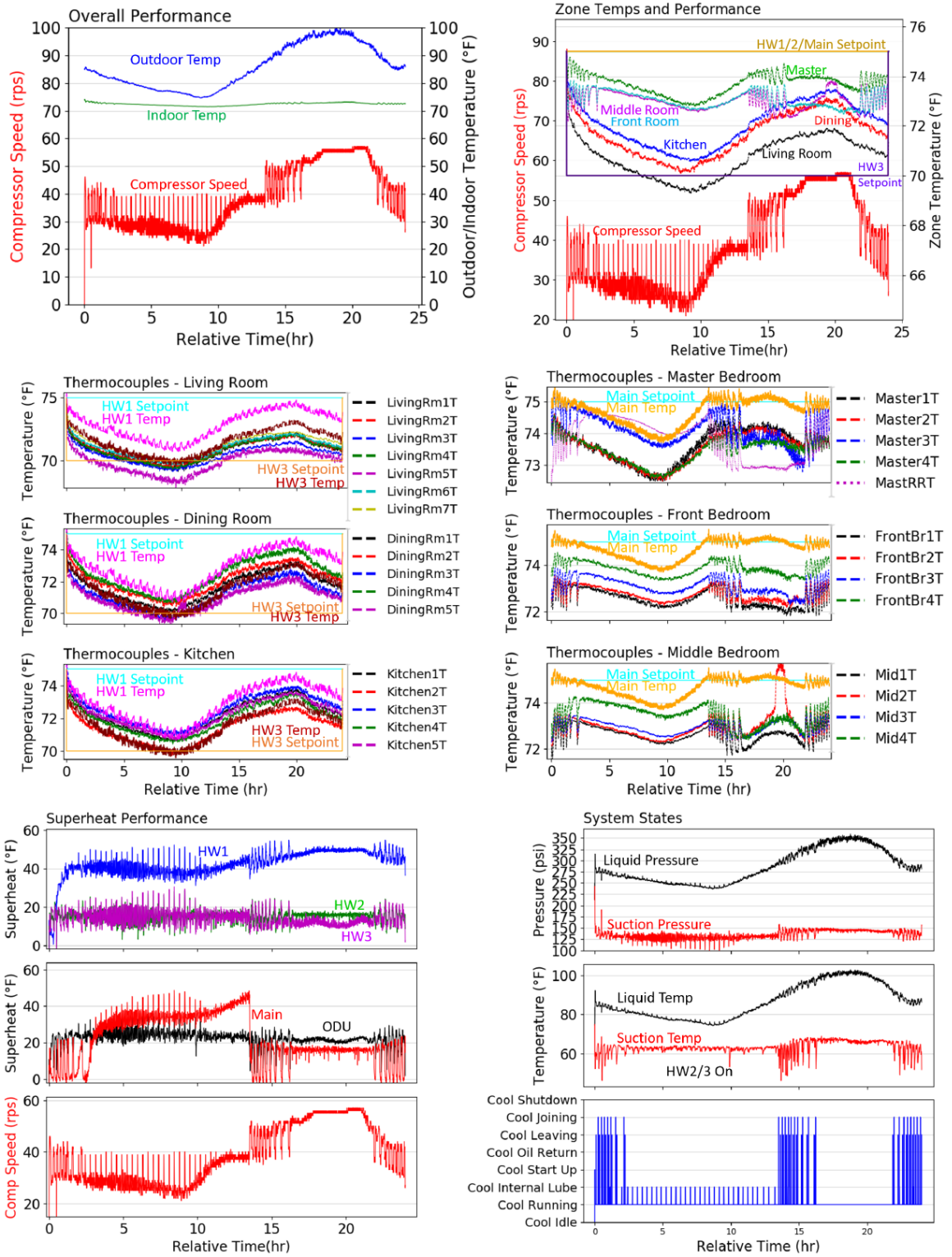


Figure D1. Scenario B data set

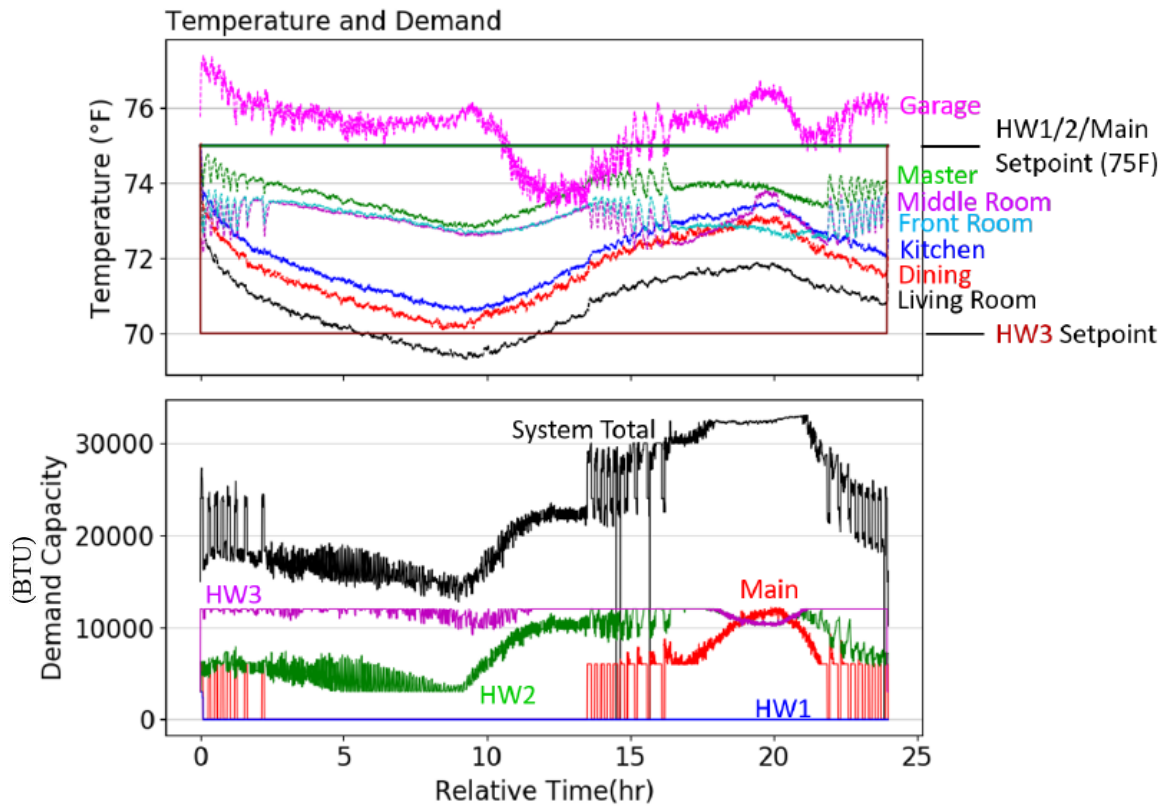


Figure D2. Scenario B data set (continued)

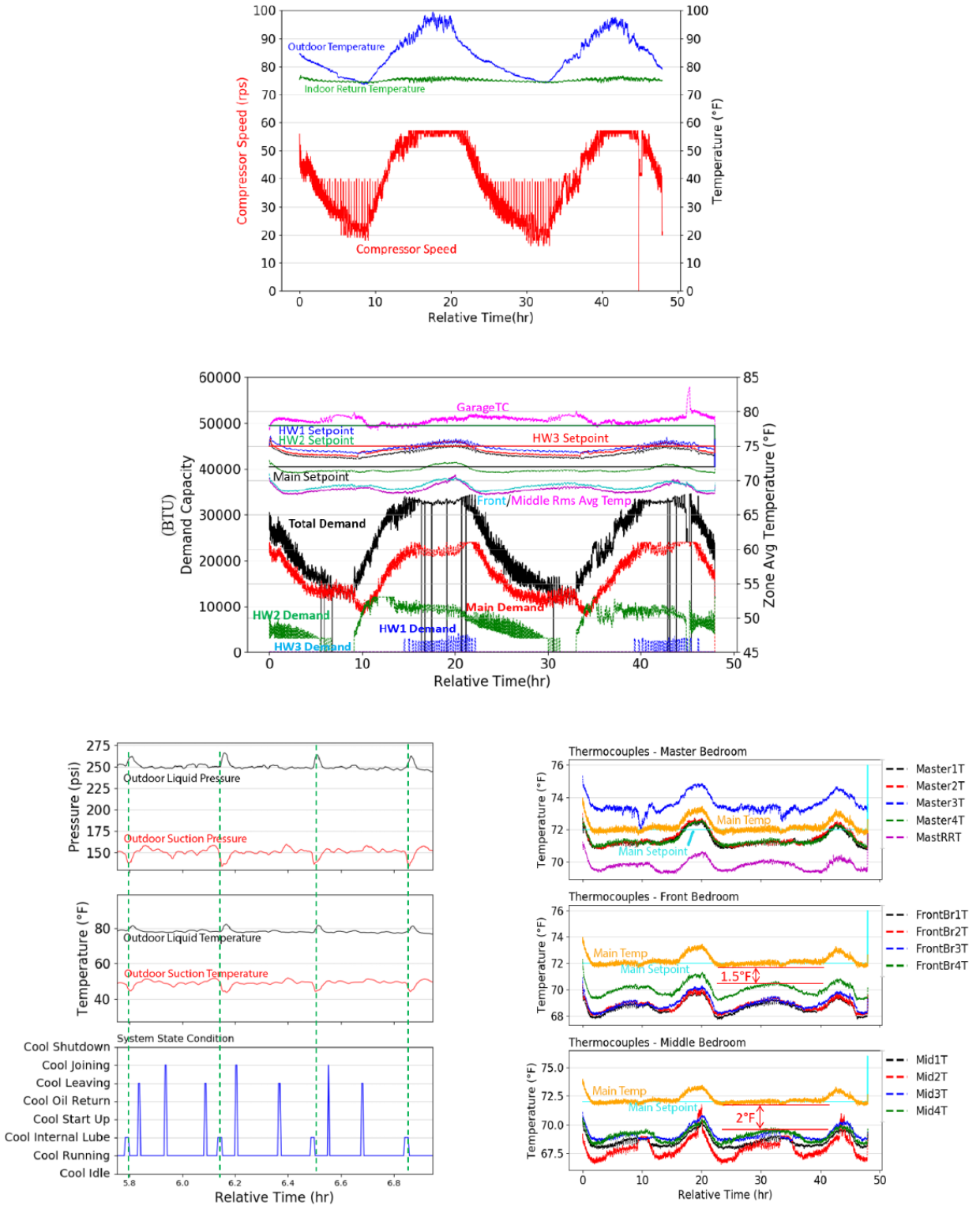


Figure D3. Scenario D data set

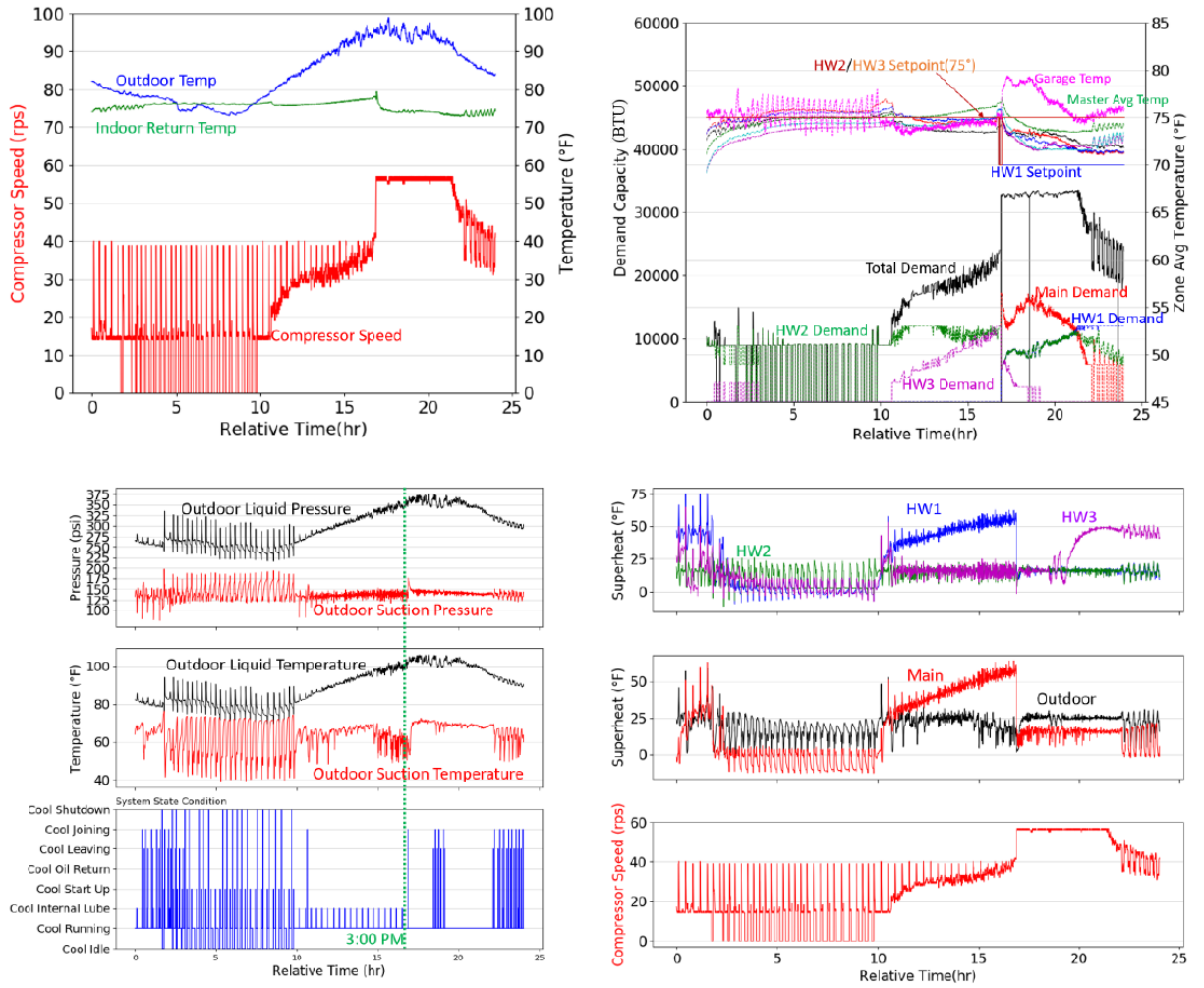


Figure D4. Scenario F data set

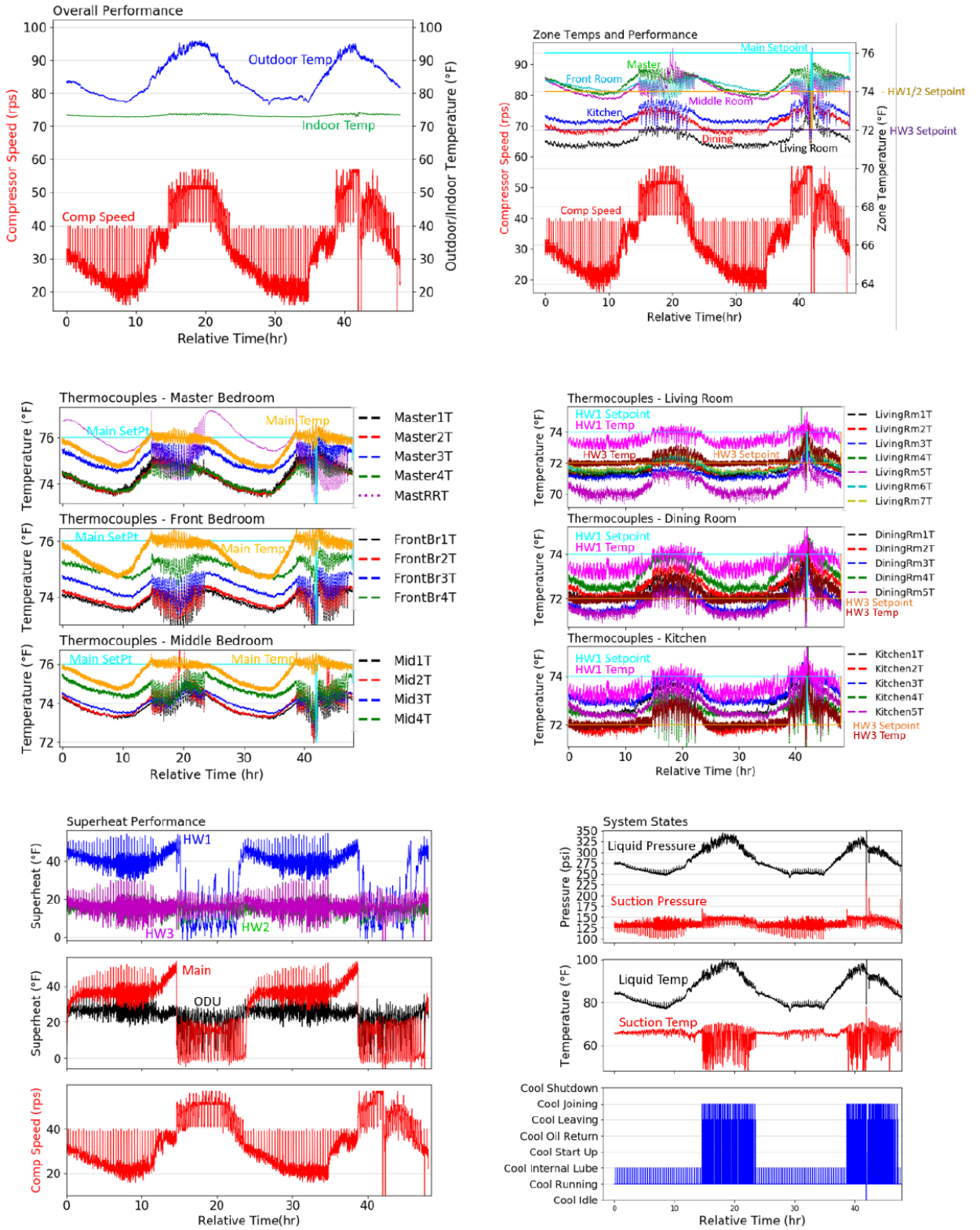


Figure D5. Scenario G data set

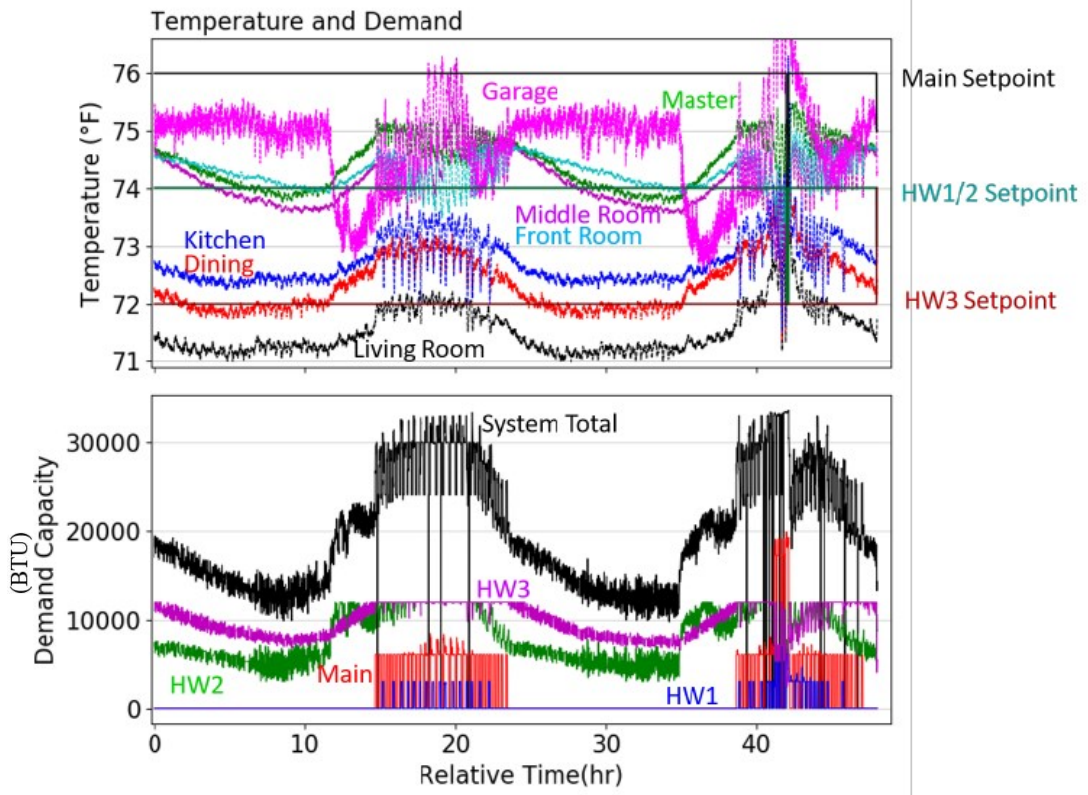


Figure D6. Scenario G data set (continued)

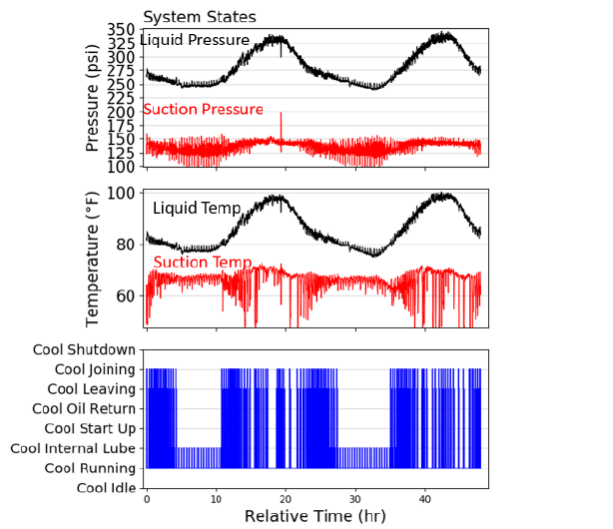
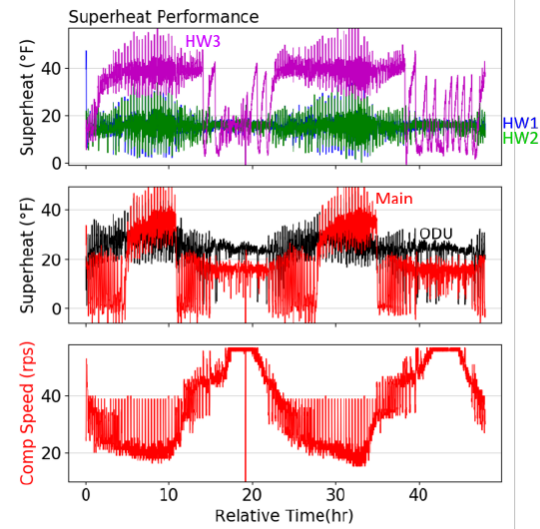
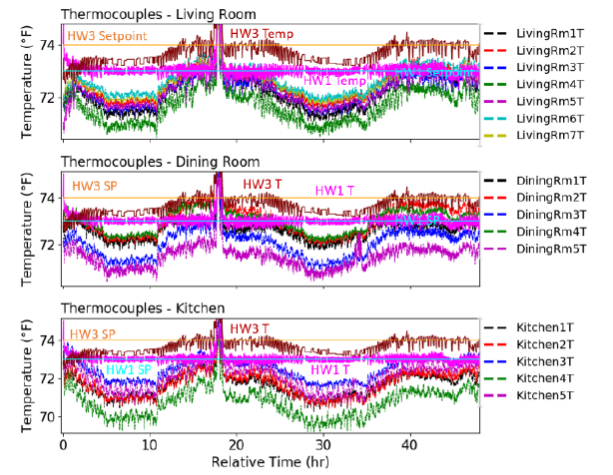
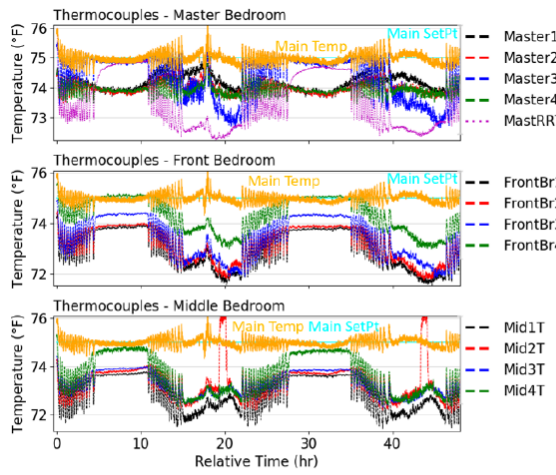
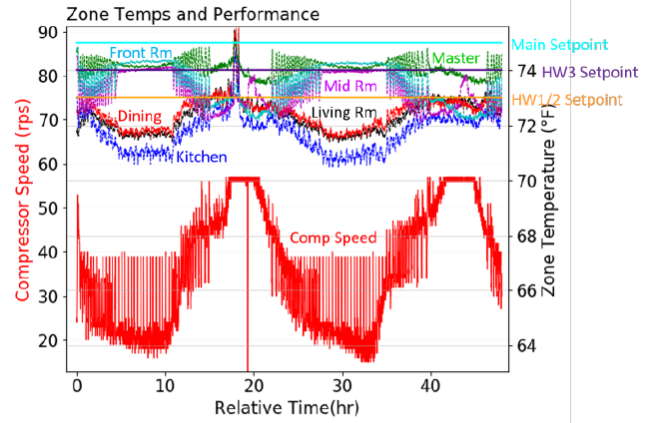
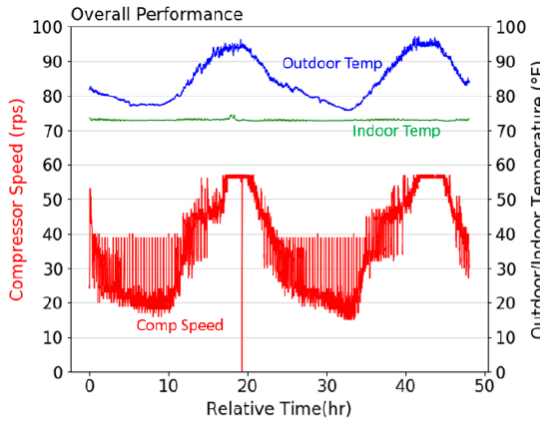


Figure D7. Scenario H data set

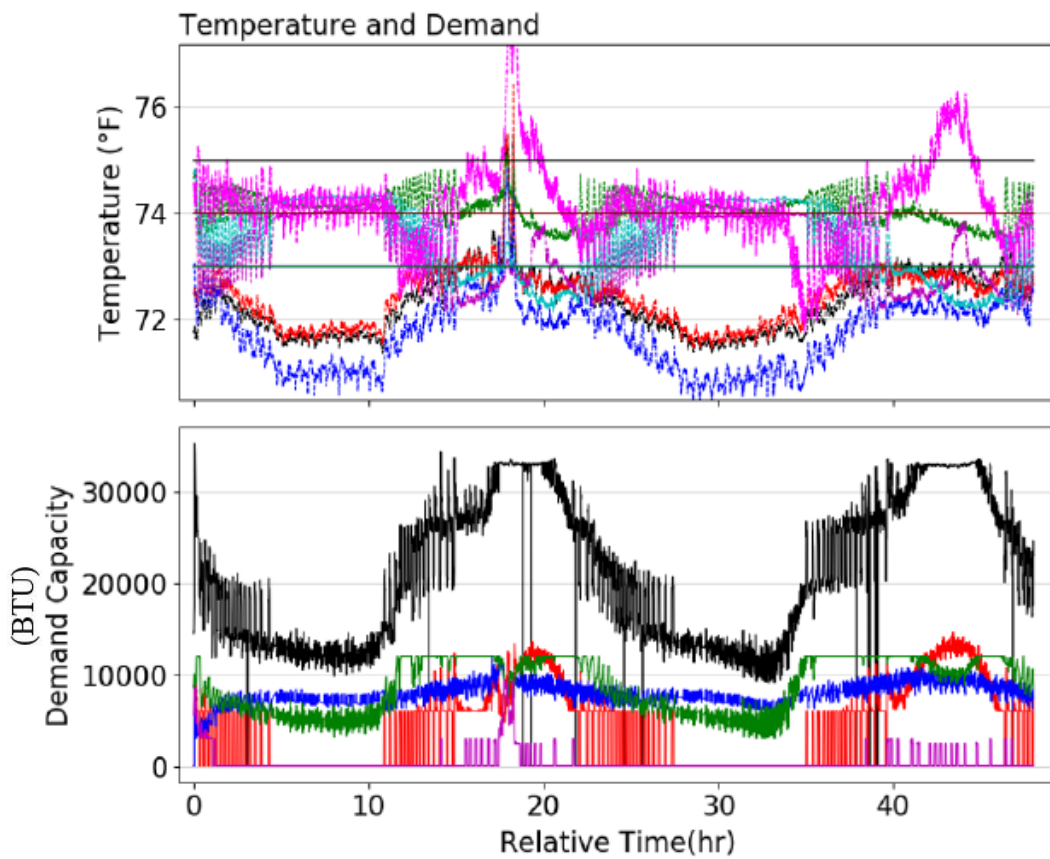


Figure D8. Scenario H data set (continued)